Coast-down and constant-speed testing of a tractor-trailer combination in support of regulatory developments for greenhouse gas emissions

McAuliffe, Brian R.; Chuang, David

Laboratory Technical Report (National Research Council of Canada. Aerospace. Aerodynamics Laboratory); no. LTR-AL-2016-0019-R, 2017-05-12

NRC·CNRC

AERODYNAMICS LABORATORY

Coast-down and Constant-speed Testing of a Tractor-trailer Combination in Support of Regulatory Developments for Greenhouse Gas Emissions

Unclassified

Unlimited

LTR-AL-2016-0019-R

May 12, 2017

Brian R. McAuliffe, David Chuang

National Research Council Canada
Conseil national de recherches Canada

Canada

AERODYNAMICS LABORATORY

Coast-down and Constant-speed Testing of a Tractor-trailer Combination in Support of Regulatory Developments for Greenhouse Gas Emissions

Report No.: LTR-AL-2016-0019-R

Date: May 12, 2017

Authors: Brian R. McAuliffe, David Chuang

Classification:	Unclassified	**Distribution:**	Unlimited
For:	ecoTECHNOLOGY for Vehicles Stewardship and Sustainable Transportation Programs Transport Canada		
Project #:	A1-007086		
Submitted by:	Dr. Steven J. Zan, **Director R&D Aerodynamics**		
Approved by:	Jerzy Komorowski, **General Manager, Aerospace Portfolio**		

Pages:	54	**Copy No:**	
Figures:	27	**Tables:**	11

Disclaimer

This report reflects the views of the authors only and does not reflect the views or policies of Transport Canada.

Neither Transport Canada, nor its employees, makes any warranty, express or implied, or assumes any legal liability or responsibility for the accuracy or completeness of any information contained in this report, or process described herein, and assumes no responsibility for anyone's use of the information. Transport Canada is not responsible for errors or omissions in this report and makes no representations as to the accuracy or completeness of the information.

Transport Canada does not endorse products or companies. Reference in this report to any specific commercial products, process, or service by trade name, trademark, manufacturer, or otherwise, does not constitute or imply its endorsement, recommendation, or favoring by Transport Canada and shall not be used for advertising or service endorsement purposes. Trade or company names appear in this report only because they are essential to the objectives of the report.

References and hyperlinks to external web sites do not constitute endorsement by Transport Canada of the linked web sites, or the information, products or services contained therein. Transport Canada does not exercise any editorial control over the information you may find at these locations.

Executive Summary

Through its ecoTECHNOLOGY for Vehicles program, Transport Canada (TC) commissioned the National Research Council Canada (NRC) to perform a verification test program of the coast-down and constant-speed test methodologies being proposed by the Unites States Environmental Protection Agency (EPA) for its second phase of greenhouse gas regulations for heavy-duty vehicles. The test program was undertaken to support combined efforts of Environment & Climate Change Canada (ECCC) and the EPA to develop the second phase of their respective greenhouse gas emissions regulations for heavy-duty vehicles. This test program acts as a site-verification exercise against testing efforts undertaken by Southwest Research Institute (SwRI) using the same ECCC-supplied tractor, as part of the US EPA regulatory development framework.

Coast-down and constant speed testing were conducted at TC's Motor Vehicle Test Centre (MVTC) using a tractor-trailer combination supplied by ECCC. The tractor was the same vehicle tested by SwRI on a rural road in Texas, and the trailer had similar specifications to those used in the SwRI tests as part of their testing for the EPA. Three vehicle configurations were tested, including the basic vehicle, the trailer outfitted with side-skirts, and the trailer outfitted with side-skirts and a boat-tail. The side-skirts were plywood replicas of the commercial product used in the SwRI tests, and the boat-tail was the same commercially-available model tested by SwRI.

The high-speed Bravo track of the MVTC was used for the test campaign. The poor condition of the track surface caused difficulties with on-board instrumentation and with the data processing. A post-test high-precision grade survey was performed to obtain adequate information to account for the track grade in the coast-down and constant-speed analyses.

A combination of track-side and on-board wind measurements were used to account for the influence of terrestrial winds on the measurements. Four track-side sonic anemometers, mounted to the sides of the track at vehicle mid-height (approx 2 m from the track surface), were used to calibrate the on-board fast-response pressure probe mounted 1 m above the front-face of the trailer (5 m from track surface). In an effort to understand better an inconsistency in some of the test results, it was shown that, conceptually, this location for the on-board wind measurement introduces error in the calibration of the wind-speed experienced by the vehicle. An on-board measurement close to vehicle mid-height would reduce errors in the test results.

Coast-down analysis of the test data was performed using two different methods. One method was the EPA-proposed High-Low Iteration method, and the second was a conventional Regression method. Results of the current test program, when analyzed using the EPA-proposed High-Low-Iteration method, showed zero-yaw drag-area ($C_{D0}A$) results within 5% of the EPA values for the same vehicle configurations. In an attempt to reduce the uncertainty of the

High-Low Iteration method, the low-speed speed-range used in the analysis was modified, and a speed-dependent rolling-resistance model was introduced. This combination of added fidelity resulted in reduced C_DA results (order of 5-10% lower). Using the same modeling assumptions, the Regression method and High-Low-Iteration method provide $C_{D0}A$ results with differences for each vehicle configuration no greater than 0.2%, providing added confidence in the modified version of the EPA-proposed analysis method.

The constant-speed method provided significant scatter in the results of C_DA and requires additional restriction on data validity to provide confidence in the data. These additional restrictions eliminated the higher yaw-angle data that were supposed to be the benefit of the constant-speed over the coast-down method. The response of the vehicle cruise control system to changes in the environment and track grade introduced uncertainty in the constant-speed results that required elimination of significant periods of usable data. With the additional restrictions on data validity, the $C_{D0}A$ results from the constant-speed measurements were found to agree with the equivalent coast-down results within 1% for each vehicle configuration.

Revisions from the original document published on July 12, 2016 include:

- Typographical error fixed in Equation 4.7 on age 38. Efficiency term removed from denominator and placed in numerator.
- Typographical error fixed in last paragraph on Page 42. $C_{Dp}A$ changed to $C_{D0}A$.

Table of Contents

List of Figures

List of Tables

Nomenclature

Symbols:

a, b, c	regression coefficients
A	area [m^2]
C_D	drag-force coefficient [ ]
C_{D0}	drag-force coefficient at zero yaw angle [ ]
C_{RR}	rolling-resistance coefficient [ ]
C_{RR0}	rolling-resistance coefficient at zero speed [ ]
F_{Aero}	aerodynamic drag force [N]
F_{Grade}	grade force [N]
F_{Mech}	mechanical resistance force [N]
F_{RL}	road load [N]
F_{RR}	rolling-resistance force [N]
F_{Trac}	tractive force [N]
F_z	vertical load [N]
g	gravitational acceleration constant [9.807 m/s^2]
h	elevation [m]
I	moment of inertia [kg m]
k	drag-coefficient yaw-sensitivity term [rad^{-1}]
L	vertical tire load [N]
m	vehicle static mass [kg]
m_e	effective mass [kg]
P	tire inflation pressure [Pa]
Q	dynamic pressure [Pa]
r	tire effective radius [m]
R_{RR}	ratio of rolling resistance to zero-speed value [ ]
s	position [m]
t	time [s]
U	wind speed experienced by the vehicle [m/s]
u	wind speed of terrestrial winds [m/s]
V	vehicle speed [m/s]
W	vehicle weight [N]
WAC_D	wind-averaged drag coefficient [ ]
z	vertical position [m]

α	regression coefficient, power-law exponent [ ]
β	regression coefficient
η	drive-axle-differential efficiency [ ]
ρ	air density [kg/m^3]
τ_{shaft}	shaft torque [Nm]
ψ	vehicle-referenced wind angle, yaw angle [°]
ω_{shaft}	shaft rotational speed [rad/s]

Subscripts:

avg	average value
ref	reference value

Acronyms:

CFD	computational fluid dynamics
DAQ	data acquisition
ECCC	Environment & Climate Change Canada
EPA	Environmental Protection Agency
eTV	ecoTECHNOLOGY for Vehicles
GEM	Greenhouse-gas Emissions Model
GHG	greenhouse gas
GPS	Global Positioning System
HDV	heavy duty vehicle
IMU	inertial measurement unit
LDV	light duty vehicle
NRC	National Research Council
SAE	Society of Automotive Engineers
SwRI	Southwest Research Institute
TC	Transport Canada

1. Introduction

Transport Canada, through its ecoTECHNOLOGY for Vehicles (eTV) program, undertakes testing and evaluation of new and emerging vehicle technologies. The program helps inform various stakeholders that are engaged in the development of regulations, codes, standards, and products for the next generation of advanced light-duty vehicles (LDVs) and heavy-duty vehicles (HDVs).

Environment and Climate Change Canada (ECCC) and the United States Environmental Protection Agency (EPA) are in the process of developing the second phase of their respective greenhouse gas regulations for heavy-duty vehicles. These regulations require vehicle manufacturers to demonstrate efficiency and emissions levels of the vehicles they sell for use in the US and Canada. The Greenhouse-gas Emissions Model (GEM), a simulation tool for these estimates, requires an aerodynamic input represented by the vehicle drag area ($C_D A$). The reference method to determine the drag-area, defined by the EPA in their first phase of regulations (U.S. Environmental Protection Agency and U.S. Department of Transportation, 2011) and proposed again as the reference method for the second phase (U.S. Environmental Protection Agency and U.S. Department of Transportation, 2015), is a road/track-based measurement technique called *coast-down testing*. Currently, no formal recommended practice exists for coast-down testing of HDVs. The first phase of the EPA regulations was based on an SAE coast-down procedure for light-duty vehicles (SAE J1263, 2010). The coast-down test methodology is to allow a vehicle to coast un-powered from high speed to a stop or low-speed state, from which the road load exerted on the vehicle can be determined by the vehicle deceleration rate. Assumptions about the manner in which external forces such as rolling resistance and aerodynamic drag behave with speed are then used to identify the drag area ($C_D A$) and rolling-resistance coefficient (C_{RR}) of the vehicle. Changes to the test methodology and analysis procedures are being considered by the EPA for the second phase of regulations.

The EPA is also considering introducing a constant-speed test procedure as a secondary method that has the potential to capture the aerodynamic behaviour of the vehicle under yawed wind conditions, from which an evaluation of the wind-average drag might be feasible. Constant-speed testing consists of evaluating the road-load experienced by a vehicle while moving at constant speed, by measuring the power delivered to the road through the drive wheels. Results from tests at various speeds are used to infer the behaviour of the road load with speed, from which the drag-area and rolling-resistance coefficient are calculated using similar assumptions as the coast-down technique. The constant-speed technique has been proposed as the reference method for the European Commission efforts to regulate greenhouse gas emissions (Luz *et al.*, n.d.).

The EPA contracted Southwest Research Institute (SwRI) to conduct a series of coast-down and constant-speed tests using different tractor models, different trailer models, different tire models, and different trailer-mounted drag-reduction technologies. One of the tractors tested by SwRI was supplied by ECCC. The results are being used to evaluate changes to the testing methodologies and to identify current levels of vehicle drag from which future drag-reduction

targets will be set. The EPA recognized the need for additional verification efforts to ensure the selected test methodology can be applied by vehicle manufacturers at different sites. The current project was initiated to support this site-verification exercise.

To support this regulatory development process, TC commissioned the National Research Council Canada (NRC) to conduct coast-down and constant-speed testing at the TC Motor Vehicle Test Centre in Blainville, Quebec, using the same ECCC-owned vehicle that was tested by SwRI. The test program was designed to supplement the SwRI data set, while introducing some enhanced wind measurement technology to the on-board measurement system. Two coast-down analysis methods were evaluated as part of the project: one that is based on conventional regression techniques; and one that has been recommended by a vehicle manufacturer and that is mathematically simpler to implement. Two variants of a constant-speed analysis were also evaluated, with results for only one presented herein.

This report documents the test procedures, the analysis methods, and the results from the coast-down and constant-speed test campaign. Section 2 describes the test setup, while Sections 3 and 4 present the analysis and results from the coast-down and constant-speed methods, respectively. Section 5 compares the results of the two method and discusses some additional wind-measurement considerations for reliable testing, and Section 6 provided the conclusions and a summary of the project.

2. Test Setup

2.1 Test Vehicle and Configurations

The test vehicle is a tractor-trailer combination supplied by Environment & Climate Change Canada for the test program. The tractor is a model-year 2014 International ProStar Long Sleeper and the trailer is a conventional 53 ft dry-van trailer manufactured by Manac Inc. The test vehicle is shown in Figure 2.1 with side-skirts and boat-tail installed on the trailer. The vehicle specifications are listed in Table 2.1. The tractor-trailer combination was configured according to EPA specifications (U.S. Environmental Protection Agency and U.S. Department of Transportation, 2015) for all but the position of the trailer bogie. As was required by the SwRI test campaign to accommodate the selected side-skirt device, the trailer bogie was positioned approximately 4 inches further aft than EPA specifications to avoid interference between the wheels and the side-skirts. This provides consistency with the EPA data set.

Three vehicle configurations were tested during the coast-down and constant-speed test campaigns, two of which included trailer-mounted drag-reduction technologies. Figure 2.2 shows the fully-outfitted trailer configuration, and Table 2.2 provides the specifications of each technology. The side-skirt shape tested was based on the reference side-skirt for the SwRI/EPA test program. The commercial product is no longer commercially available and therefore plywood replicas were build for the current test program. Low-profile brackets were used on the underside for mounting, with negligible structural interference with the wind to influence the vehicle drag in any measurable quantity. The three vehicle configurations tested were:

1. Baseline: no drag reduction technologies
2. Skirts: side-skirts installed
3. Skirts+Tail: side-skirts and boat-tail installed

The vehicle mass was maintained within 1.5% of its fully-loaded value of 15,796 kg throughout the test campaign. When not installed on the trailer, the side-skirts and boat-tail were stored inside the trailer to maintain weight. The fuel level was maintained at 3/4 full or greater throughout testing. Based on records of fuel fill-ups and estimates of fuel use during the test campaign, the vehicle mass for each coast-down or constant-speed run has been calculated for use during data processing, with an estimated uncertainty of $\pm$25 kg. No ballast was used in this test program.

2.2 Test Site

Testing was performed at the Motor Vehicle Test Centre operated by PMG Technologies in Blainville, Quebec. The “Bravo” track was used for testing, highlighted in green in the aerial photograph of Figure 2.3. The “Bravo” track is the high-speed banked oval and the primary

Figure 2.1: Photograph of the test vehicle.

Figure 2.2: Photograph of the trailer configured with side-skirts and a boat-tail.

Table 2.1: Tractor-Trailer specifications.

Tractor	Chassis: Navistar ProStar AR+ 122; 2013 VIN: 3HSDJSNR0EN785904 Engine: 2013 Navistar N13; A450MT (450 HP 1700 RPM) Transmission: Eaton UltraShift PLUS LSE Tandem drive (6×4) Meritor MT-40-14X-4CFR
Trailer	Manac 53 ft dry-van Model 94253A111 Unit 141951 tandem-axle bogie
Tires	Steer: 2 × Hankook AL-11 295/75R22.5 loaded radius (L/R) 473 / 477 mm cold inflation pressure 124 ±7 psi Drive: 8 × Bridgestone M-710 295/75R22.5 forward loaded radius (L/R) 503 / 510 mm aft loaded radius (L/R) 503 / 508 mm cold inflation pressure 107 ±5 psi Trailer: 8 × Bridgestone R-197 295/75R22.5 forward loaded radius (L/R) 503 / 510 mm aft loaded radius (L/R) 503 / 508 mm cold inflation pressure 105 ±5 psi
Weight and Dimensions	15,796 kg (as tested, fully fueled) Overall Height (H101) = 4.115 m (162.0 in) Overall Width (W103) = 2.600 m (102.3 in) Frontal area = 10.699 m^2 Tractor-trailer gap width: 1.79 m (45.5 in) at ≈1.5 m height 1.81 m (46.0 in) at ≈2.5 m height Trailer rear axle = 2.95 m (116 inch) from back of trailer Trailer inter-axle spacing = 49 inch King-pin location 0.91 m (36 in) from front of trailer

Table 2.2: Drag-reduction-technology specifications.

Name	Description
Skirts	Plywood replica commercial side-skirt design Flush with sides of trailer sides Length = 8.66 m (341 in), Height = 0.927 m (36.5 in) 45°taper on front and back edges
Tail	Collapsible commercial boat-tail 4-panel configuration (sides + top + bottom) Extension from rear of trailer = 1.2 m (48 in)

surface is rain-grooved concrete. The track is 6.5 km (4.0 miles) long with two straight 1.6 km (1.0 mile) sections. A small segment of the north-side straight section has been repaired using asphalt, identified with a purple line in Figure 2.3.

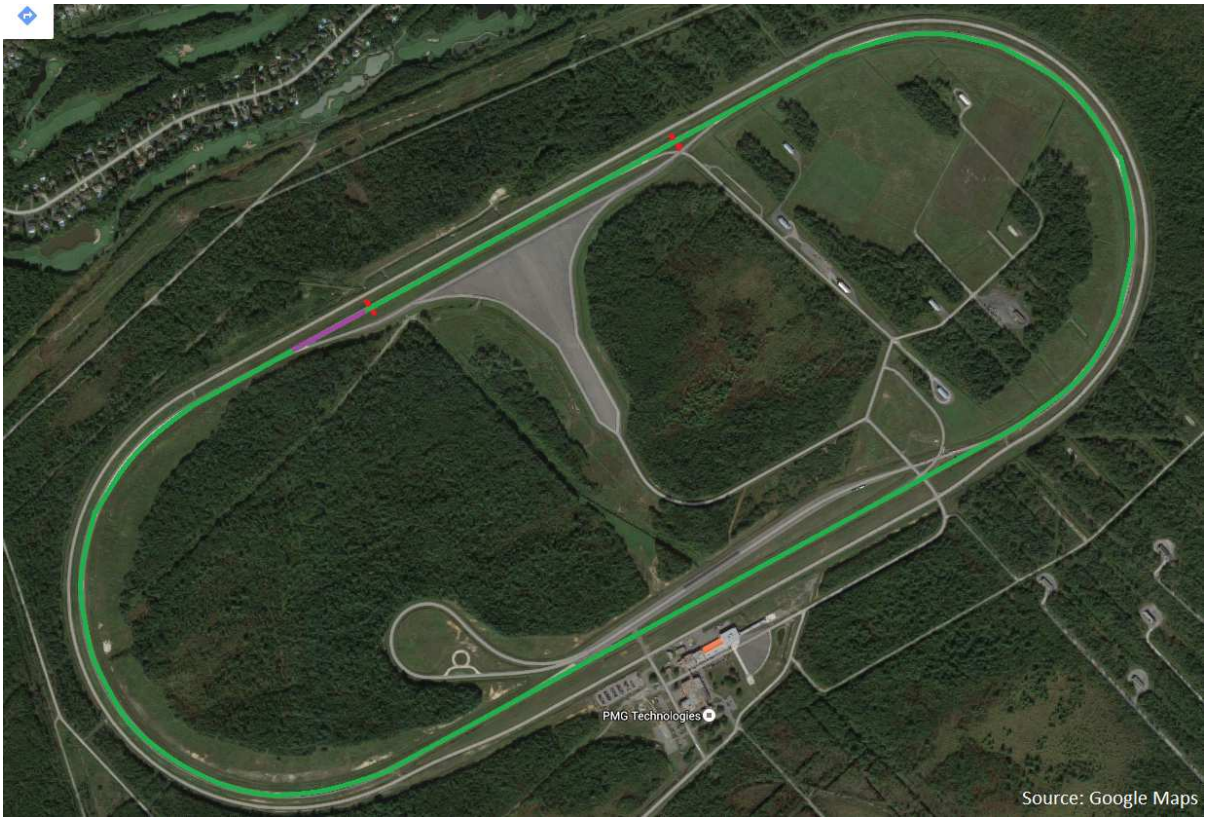

Figure 2.3: Aerial view of the motor Vehicle Test Centre ("Bravo" track highlighted in green with asphalt section highlighted in purple, anemometer locations identified by red dots, photo adapted from Google Maps).

The track grade can have an influence on the results of coast-down and constant-speed tests. The EPA requires grade to be accounted for if it exceeds 0.02% (U.S. Environmental Protection Agency and U.S. Department of Transportation, 2011). Initially it was anticipated that the high-speed GPS elevation data from the on-board instrumentation would provide, based on a long-term average over the duration of the test program, a reasonable measure of the grade profile for use in the data analysis. Unfortunately, instrumentation problems early in the test prevented the detailed elevation data from being acquired. A single day of elevation data collected with the high-speed GPS is available, but low-frequency drift in the signal provided insufficient data to characterize the absolute grade profile for the two straight sections of the track. However, good repeatability of the "bumpiness" profile of the track was obtained from this data set by applying a high-pass spatial filter with a 200 m filter cut-off. To obtain elevation data of the track, from which the absolute grade could be defined, a precise but low-resolution elevation survey of the track was completed in December 2015, comprising track elevation data at 100 m spacing along the length of the track. To obtain a high-resolution ab-

solute elevation profile of the track, the "bumpiness" profile measured by the single-day of high-speed on-board GPS data was combined with the precise low-resolution elevation survey data. Figure 2.4 shows the high-resolution elevation survey for the north side of the track and the low-resolution elevation survey of the south side of the track. The north side has a consistent grade but with local bumpiness. The south side has two segments of consistent but near opposite grade. The south-side data in Figure 2.4 does not show the bumpiness profile. Its bumpiness has similar spacing as the north side but with approximately half the amplitude of the bumps.

For coast-down and constant speed analyses, the magnitude of the grade is important. Figure 2.5 shows grade profiles based on elevation profiles of different resolution for the track. The north-side data shows the high-resolution grade profile in black that accounts for the track bumpiness. Although the nominal grade is on the order of 0.05%, locally the grade can exceed a magnitude of 0.2%. The bumps in the track may cause vertical accelerations of the vehicle but will not necessarily introduce a grade force in the direction of motion of the vehicle because the vehicle's weight is distributed over a much greater horizontal extent than the bump. Therefore, a low-pass spatial filter with a cut-off of 25 m was used to represent the grade that would be felt by the vehicle. The low-resolution (low-res) profile for the north-side grade represents the filtered version of the high-resolution profile. The south-side low-resolution grade profile represents similarly filtered data.

All coast-down runs were performed on the north side of the track due to its low nominal

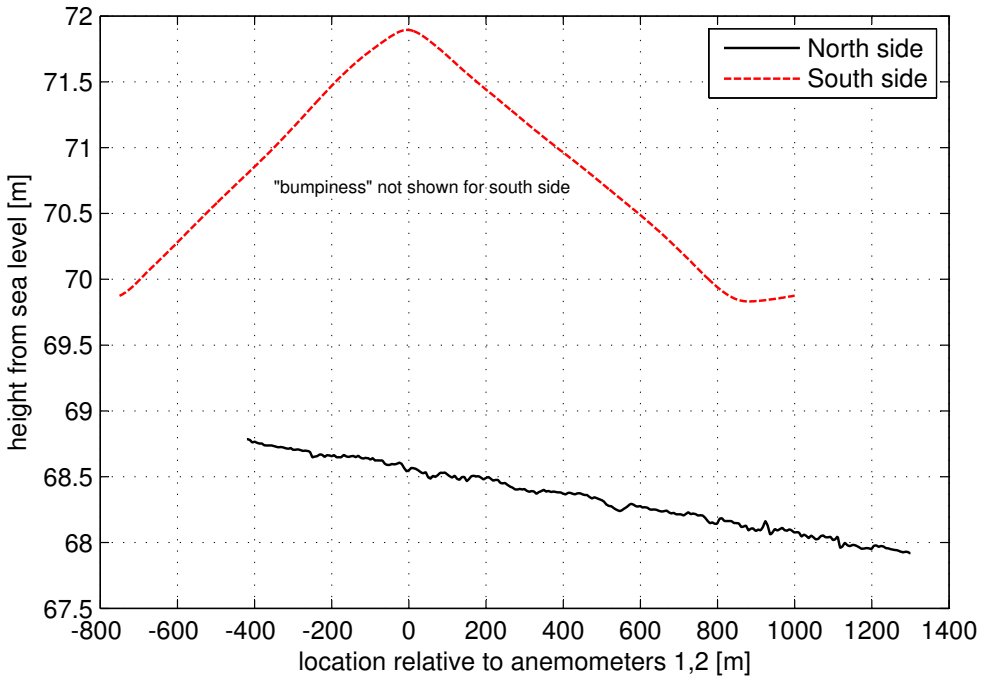

Figure 2.4: Bravo track elevation profile.

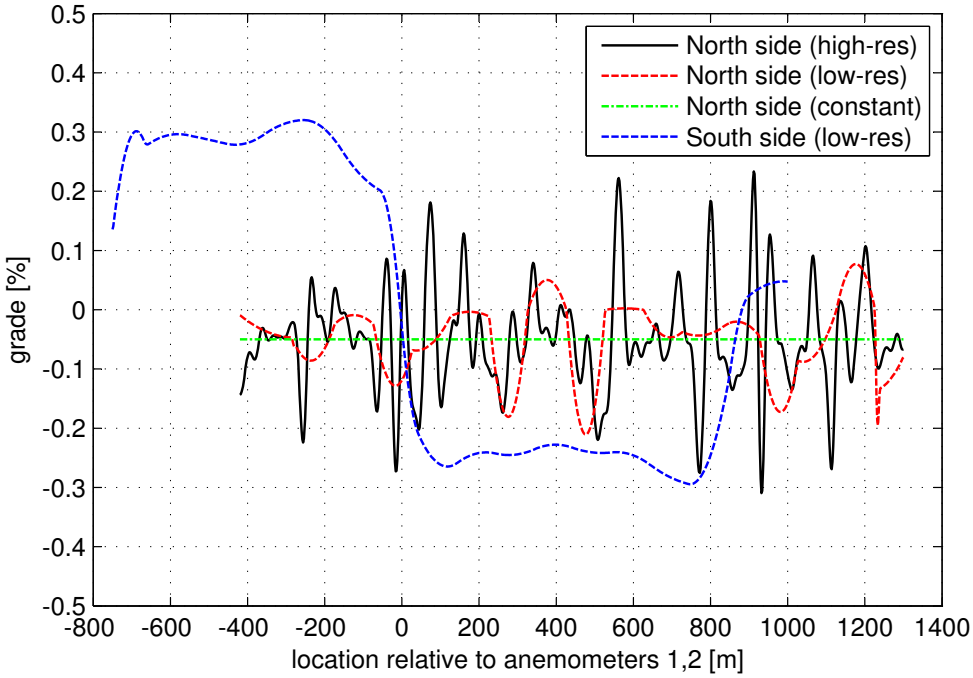

Figure 2.5: Bravo track grade profile.

grade.

2.3 Instrumentation and Data Acquisition

The measurement requirements for the coast-down and constant-speed test campaigns were as follows:

- Vehicle position
- Vehicle speed
- Driveshaft torque (for constant-speed measurements only)
- Driveshaft speed (for constant-speed measurements only)
- Air properties (temperature and barometric pressure)
- Wind conditions (speed and direction, as experienced by the vehicle)

Vehicle speed and position were measured by an on-board GPS system. The system is a Speedbox RTK IMU unit by *Race Technology*, which uses a built-in inertial measurement unit (IMU) to augment the conventional GPS signal and provide a higher update rate than the conventional GPS signal alone could provide. Other vehicle-specific parameters such as gear selection, in-

dicated speed, engine temperature, and other data available on the vehicle network were also recorded using a J1939 datalink. Some of this data, such as gear selection, were useful to identify measurement segments of interest. The high-speed GPS data and the vehicle-parameter date were acquired at 100 Hz, whereas the conventional GPS data was acquired at 5 Hz.

For the constant-speed measurements, the driveshaft torque was measured using a HBM Model T40B shaft torque meter loaned to NRC by SwRI. This instrument was the same device used by SwRI for their test campaign with the ECCC ProStar vehicle. It including a modified driveshaft as prepared by SwRI. After completion of testing, the connection between the modified driveshaft and the torque meter was found to be loose. Broken and loose bolts were found, and a misalignment at the connection was observed, however there was no wobble in the system. Post-test checks of the connection and some low-speed coast-downs were performed to check for possible adverse effects on the coast-down tests, but no concerns were raised. The drive-shaft torque measurements showed high fluctuations in the signal ($\pm$50% peak-to-peak) throughout the entire test campaign, higher than those observed in the SwRI data. These fluctuations are associated with a distinct frequency of 7 Hz regardless of vehicle speed (dominant frequency at 16 km/h is the 3.5 Hz sub-harmonic), and are therefore not expected to be associated with the loose driveshaft. The similarity in results between the two methods described in this report, and similarity to the SwRI/EPA results, indicates that the loose driveshaft did not cause any adverse effects on the data presented in this report. The driveshaft data were acquired at 100 Hz. The SwRI data was acquired at 10 Hz and it is unclear whether any pre- or post-filtering of the data was performed.

The wind conditions experienced by the vehicle were measured using a fast-response four-hole pressure probe that measures the fluctuations in wind speed, wind direction, and pressure. This "Cobra probe" is manufactured by *Turbulent Flow Instrumentation Pty Ltd*. The probe has pressure transducers build into the stem which, combined with the short length of tubing between the probe tips and the transducers, allows correction for the frequency response of the system with a resolution up to 1.5 kHz, above which the on-board electronics filter the output signals. For the majority of measurements presented herein, the measurement uncertainties for the wind speed and turbulence intensity are within $\pm$0.5% of measured values, and the flow angle uncertainties were within $\pm 1^\circ$, based on a pre-test calibration verification in the NRC 1.0 m $\times$ 0.8 m Pilot Wind Tunnel. The reference-pressure port of the Cobra probe was connected to the static port of a pitot-static probe mounted in close proximity to the Cobra probe. This reference pressure was also measured by an absolute pressure transducer to allow calculation of the air density from the local static pressure. The Cobra-probe data were acquired at 2 kHz.

Figure 2.6 shows the installation of the Cobra probe and the pitot-static probe on the front of the trailer. The Cobra probe was mounted 1.0 m above the trailer roof with its tip 0.3 m forward of the front face of the trailer. The pitot-static probe was mounted such that its static-pressure ports were 0.3 m below the tip of the Cobra probe.

The Cobra probe was mounted sufficiently close to the vehicle (1.0 m above the trailer) such that its measurement of wind speed and direction do not represent the true wind speed and direction experienced by the vehicle. To provide a means of calibrating the on-board measurement for this vehicle-proximity influence, four sonic anemometers were installed along at

Figure 2.6: Wind-measurement probes mounted to front face of the trailer (Cobra probe - high, pitot-static probe - low).

Figure 2.7: Track-side sonic anemometers.

two locations on north side of the track with one on each side of the track (see locations in Figure 2.3). The anemometers used were R. M. Young Company model 81000 3-D ultrasonic anemometers and were mounted on tripods with the sensing element elevated to be coincident with the test vehicle's mid-height dimension, which was approximately 2.05 m above the track surface. The anemometers were located to the sides of the track 8 m from the track centerline. The anemometers were oriented to provide orthogonal wind velocity components aligned to the vehicle travel direction so as to provide a direct reading of headwind and cross-wind components. Alignment of the track-side anemometers is estimated to be within 2° of the desired orientation. Figure 2.7 shows the installation of the track-side anemometers.

The track-side data acquisition systems were installed inside weather-resistant cases located beside each anemometer. The system consisted of a data acquisition system, appropriate cables, connectors, 12 VDC deep-cycle lead-acid battery, and a 120 VAC power inverter. Data acquisition was started and stopped manually for each running direction. The data acquisition system had a quick-look capability so that the test engineer could review the results of each series of tests to evaluate nominal wind levels during the tests. The track-side anemometers have a maximum sampling rate of 32 Hz, but were up-sampled to 100 Hz for synchronization with the vehicle data.

The tractor data acquisition system was installed inside the cab of the tractor. The system consisted of a laptop, a data acquisition system, software and appropriate cables, connectors and a power supply. As part of the data processing process, all data was either up-sampled or down-sampled to match the 100 Hz acquisition rate for the vehicle speed measurement. The data from the four track-side acquisition systems were synchronized using the GPS time stamp. The 5 Hz GPS update rate thus provides an accuracy on synchronization to the tractor-based data to the track-side anemometer data of 0.2 s.

2.4 Wind Limits and Calibrations

Generally wind constraints are imposed for track-based test procedures to minimize the influence of the winds on the measurements. For the current test program, the enhanced wind-measurement capabilities provide the potential to capture and account for wind effects to a greater extent than typical track-based tests. These data can also serve to test the viability of existing procedures vis a vis maximum wind speed. For the current test campaign, standard SAE wind limits, per the J1263 coast-down procedure (SAE J1263, 2010) were targeted for a specified number of measurement runs, with a set of expanded wind limits specified for additional testing if time permitted. The J1263 and the expanded wind limits are tabulated in Table 2.3. The winds for the majority of the test program were within the J1263 limits, in large part due to the the dominant winds of the Blainville region being aligned with the track direction. Furthermore, the forested areas surrounding the track and in the middle of the track act to channel the winds along the straight sections. As such, any strong winds resulted in predominantly head- or tail-winds for the vehicle with very few conditions encountered with strong cross-winds. This limited the ability to capture high yaw angles of the wind relative to the vehicle.

Table 2.3: Wind limits for the test campaign.

Component	SAE J1263 limit	Expanded limit
average wind speed	16 km/h (10 mph)	20 km/h (12.4 mph)
peak wind speed	20 km/h (12.4 mph)	25 km/h (15.5 mph)
average cross-wind speed	8 km/h (5 mph)	14 km/h (8.7 mph)

As noted in the previous section, the on-board wind measurement (Cobra probe) was mounted sufficiently close to the vehicle (1.0 m above the front face of the trailer) that the wind-speed and angle measurements do not represent the true freestream conditions. To correct for this vehicle-proximity influence, the on-board wind measurement was calibrated against the track-side wind measurements. In the presence of terrestrial winds, the calibration of the on-board to the track-side measurement can only be done when the vehicle is in close proximity to the track-side anemometer of interest. For the purpose of the current test campaign, the data for all valid coast-down and constant-speed runs was processed and the on-board and track-side wind measurements were each averaged during the period over which the anemometer was within the range 2 m and 12 m of the vehicle position along the track direction. This range provided a period of data during which the vehicle was sufficiently close to the anemometers without the aneometers feeling the influence of the passing vehicle vehicle. Other more advanced techniques are available for calibrating the on-board wind measurement, such as the Taylor-hypothesis method implemented by Tanguay (2012) which accounts for the advection of turbulence in the terrestrial winds, and is suitable when the anemometer is located far from the track. For the current test campaign, the track-side measurements were sufficiently close to the track (8 m from track centreline) that an average of the anemometer measurements on the two sides of the track have been used as a measure of the winds the vehicle experiences when in the range 2-12 m ahead of the vehicle. Furthermore, the height differential between the on-board and track-side measurements (2 m and 5 m, respectively) can introduce some uncertainty in the turbulence-advection method because the wind speed and angle change with height relative to the vehicle in a sheared terrestrial boundary-layer wind. A discussion of this shear influence and its potential impact on the accuracy of the results is discussed in a later section of this report (Section 5.2).

Recent wind-tunnel measurements have been performed in the NRC 9 m Wind Tunnel using its 30%-scale tractor-trailer model for which a Cobra probe was placed at a similar location relative to a tractor-trailer model (1 m above the trailer front face) and compared to measurements from a Cobra Probe located sufficiently far upstream of the vehicle to ensure freestream wind conditions. These measurements showed a negligible influence of yaw angle on the speed calibration for the on-board probe, and showed a linear relationship between the on-board yaw measurement and the freestream wind direction. It has been assumed for the purpose of the current study that these trends are consistent with the vehicle on the track. Based on a few restrictions on the difference between the opposing track side anemometer measurements and differeces from the track-side to the on-board measurements, a large data set of 518 data points collected over the entire test campaign were used to develop a calibration between the

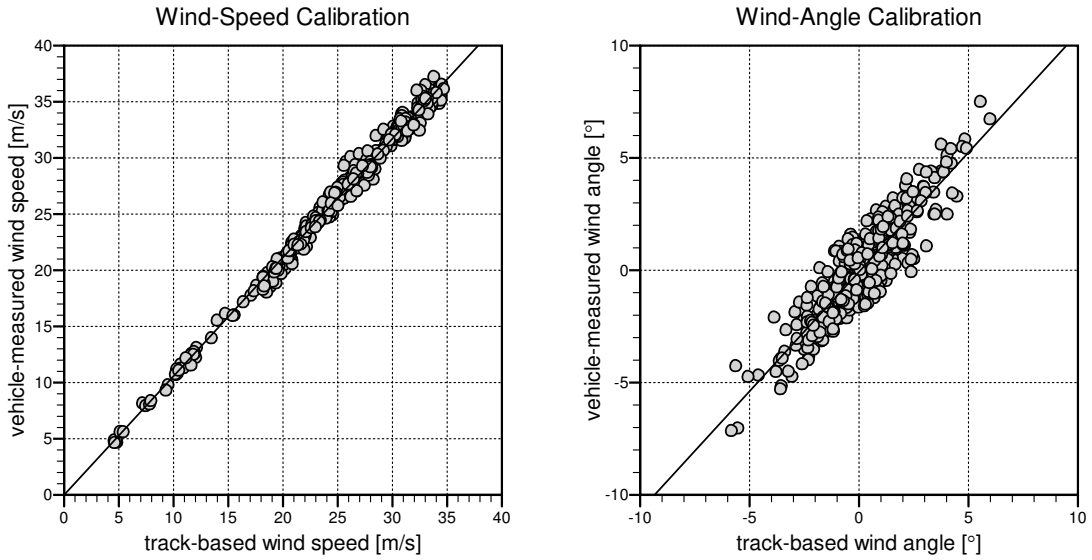

Figure 2.8: Calibration data between on-board and track-side wind measurements (left - wind speed, right - yaw angle).

on-board Cobra-probe measurement and the track-side anemometers. The calibration of wind speed and yaw angle are shown in Figure 2.8. From this data, the calibrations are:

$$U_{wind} = 0.946\, U_{probe} \tag{2.1}$$

$$\psi_{wind} = 0.94\, \psi_{probe} + 0.07 \tag{2.2}$$

The offset in the yaw angle calibration is small but it is consistent with an offset observed in a pre-test calibration verification of the Cobra probe using the NRC 1.0 m $\times$ 0.8 m Pilot Wind Tunnel.

3. Coast-Down Method

3.1 Test Procedures

The coast-down tests were performed on the "Bravo" track at the Motor Vehicle Test Centre operated by PMG Technologies in Blainvile, Québec. The tests were performed with the vehicle and instrumentation as described in Section 2. Pre-run inspections and checks were conducted to ensure that the vehicle condition was consistent from test to test. Specific items checked included:

1. Cold tire inflation pressure;
2. Doors and windows were fully closed;
3. HVAC and A/C settings remained consistent; and
4. Fuel level at least 3/4 full.

Prior to the start of testing, the vehicle was warmed up by driving normally for several laps of the track. During this time, the track-side instrumentation was initialized and checked.

The general procedure to be followed for this test is covered by one or more of the following documents:

- US CFR Title 40, Section 1066.310, "Coastdown procedures for heavy-duty vehicles" (U.S. Environmental Protection Agency and U.S. Department of Transportation, 2011)
- SAE J1263, "Road load measurement and dynamometer simulation using coastdown techniques" (SAE J1263, 2010)
- SAE J2263, "Road load measurement using onboard anemometry and coastdown techniques" (SAE J2263, 2008)

Procedurally, the vehicle was accelerated to above the desired entry speed and allowed to coast in a straight line to a full stop. The vehicle was driven in both directions on the north section of the track in order to capture wind and grade variations in different directions.

The test procedure used for the coast-down tests were as follows:

1. Data acquisition system was started. The Cobra probe was zeroed.
2. The vehicle was accelerated to the required entry speed for the speed range being tested. This speed was held constant as the vehicle entered the test area.
3. The vehicle's travel direction was straightened. The throttle pedal was then released and the transmission was shifted into neutral.
4. The coastdown runs were split into three speed ranges: high-range, mid-range, and low range portions. A complete run in one direction consists of a high-range, low-range and

occasionally a mid-range run. Mid-range data were specified for only two runs in each direction for every trailer configuration.

a) For the high-range portion, the vehicle was accelerated to an entry speed of 115 km/h. Preliminary test runs showed that the vehicle would coast to an exit speed of approximately 70-75 km/h, depending on the trailer configuration. The high-range portion was conducted for every coastdown set.

b) For the low-range portion, the vehicle was accelerated to a speed above 50 km/h and allowed to coast to a full stop. The low-speed segment was conducted for every coastdown set.

c) For the mid-range portion, the vehicle was accelerated to an entry speed of 80 km/h. Preliminary test runs showed that the vehicle would coast to an exit speed of approximately 30-35 km/h, depending on the trailer configuration. The mid-range segment was only performed twice for each trailer configuration.

5. Steps 2 through 4 inclusive were repeated at least seven times.

6. After the runs were completed, the DAQ system was stopped and the recorded data saved.

7. The running direction was then reversed and steps 1 through 6 inclusive were repeated.

Only the north side of the "Bravo" track was used for the coast-down runs.

3.2 Test Conditions

The track consists of 1.6 km straight sections, which are not of sufficient length to perform a full coast-down from 112 km/h (70 mph) to near-zero speeds. As described in the previous section, the coast-down runs were segmented into three speed ranges, defined approximately by the following target intervals:

- High-Speed: 112-64 km/h (70-40 mph)
- Medium-Speed: 80-32 km/h (50-20 mph)
- Low-Speed: 48-0 km/h (30-0 mph)

For the coast-down data analysis, high-speed and low-speed data were the most important, therefore a smaller number of medium-speed-range data was collected. For each vehicle configuration, a target of 14 high/low-speed data runs were specified (7 in each direction). Table 3.1 lists the total number of coast-down runs performed during the test program for each of the three vehicle configuration. More runs were acquired for the Skirts configuration in an attempt capture a greater range of wind angles by testing in windier conditions.

Table 3.1: Test matrix for coast-down runs (SW - south-west direction, NE - north-east direction).

	Low Speed Runs		Medium Speed Runs		High Speed Runs	
	SW	**NE**	**SW**	**NE**	**SW**	**NE**
Baseline	8	8	2	2	8	8
Skirts	11	9	2	2	16	10
Skirts+Tail	9	9	1	1	9	9

3.3 Coast-Down Analysis

3.3.1 Equation of Motion

The concept of coast-down analysis is to infer the external forces (road load) acting on a vehicle based on its un-powered deceleration, and inferring the various components of the road load based on an understanding of the manner in which such forces change with time or speed. Figure 3.1 shows a pseudo free-body diagram of an un-powered vehicle during a coast-down. The forces that resist or impact forward motion to the vehicle are:

- Aerodynamic Drag (F_{Aero}) - resistive force as the vehicle moves through the air;
- Rolling Resistance (F_{RR}) - resistive force due to deformation of the tire material at the interface with the ground;
- Mechanical Resistances (F_{Mech}) - Resistance to motion due to friction within mechanical components such as bearing or differentials; and
- Grade Force (F_{Grade}) - component of the vehicle weight in the direction of motion due to the grade/inclination of the road surface from horizontal.

The aerodynamic drag, rolling resistance and grade force contribute to the Road Load (F_{RL}), which is the combination of external forces acting on the vehicle while in motion. The mechanical forces are internal to the vehicle system but must be accounted for as they contribute to the declaration of the vehicle through the rotating drive-train components downstream of the transmission.

Applying Newton's 2^{nd} law of motion in the direction of motion of the vehicle, the resulting equation is

$$m_e \frac{dV}{dt} = -F_{Aero} - F_{RR} - F_{Mech} - F_{Grade} \tag{3.1}$$

from which the change in vehicle speed (V) with time (t) is related to the resistive forces described above.

In Equation 3.1, the m_e term is the effective mass of the vehicle, which differs from the static mass of the vehicle. The rotational inertia of the wheels is a property that inhibits changes to

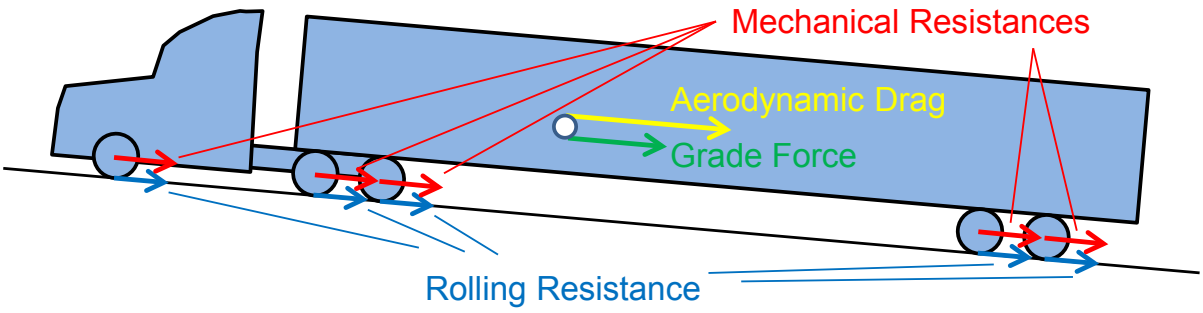

Figure 3.1: Free-body diagram of a vehicle in a coast-down.

the speed of the wheels, and behaves in an equivalent manner as the vehicle mass that inhibits changes to the speed of the vehicle. The effective mass associated with the rotating wheels is defined as

$$m_{e,wheels} = \sum_{i=1}^{N_w} \frac{I_i}{r_i} \tag{3.2}$$

where I_i is the moment of inertia of the i^{th} wheel, r_i is the radius of the loaded wheel (distance from rotational axis to the ground), and N_w is the number of wheels on the vehicle. The effective mass of the vehicle is therefore

$$m_e = m + m_{e,wheels} \tag{3.3}$$

For the purpose of this project, a typical value for the effective mass of each wheel of 56.7 kg has been used, based on measurements performed by the EPA for SmartWay verified tires with conventional steel-rims. The effective mass of all 18 wheels on the vehicle is therefore estimated to be 1020.6 kg, which is 6.5% of the static vehicle mass. As an example of the uncertainty of using a predefined value for $m_{e,wheels}$, an error of approximately 16% on the effective mass of the wheels would result in a 1% error on the road load.

The aerodynamic drag force is the parameter of most interest for the current investigation. The drag force for a vehicle can be defined as

$$F_{Aero} = Q\ C_D\left(\psi\right)\ A \tag{3.4}$$

where the dynamic pressure of the wind (Q) is dependent on the air density (ρ) and wind speed relative to the vehicle (U):

$$Q = \tfrac{1}{2}\ \rho\ U^2 \tag{3.5}$$

In Equation 3.4, the drag coefficient (C_D) is shown as a function of yaw angle (ψ - wind angle relative to the vehicle). The drag coefficient of heavy-duty vehicles has been shown to have a dependence on Reynolds number and therefore changes with wind speed. Recent data shows that, for modern aerodynamic tractor-trailer combinations, the greatest influence of C_D to Reynolds number occurs at low speeds ($\lessapprox$50 km/h) for which the drag force is small due to the low dynamic pressure (Wood, 2012; McAuliffe and Kirchhefer, 2015). As such, this Reynolds-number dependence can be neglected without introducing a measurable error into the analysis.

For the coast-down analyses presented in this report, the results will be presented by the drag-coefficient area ($C_D A$), also called the drag area, which precludes the requirement for an accurate measure of the vehicle frontal area. Drag area is useful for direct vehicle-to-vehicle comparisons when full-scale vehicles or models are used, as it represents the ratio of drag force to dynamic pressure without any requirement for geometric information.

The rolling resistance (F_{RR}) of a tire can be affected by many factors such as vertical load on the tire, inflation pressure, rotational speed, and ground texture. In conventional coast-down testing, such as the SAE J1263 procedure, it is assumed that only vertical load influences the rolling resistance, and that all tires on the vehicle behave in the same manner such that a constant rolling-resistance coefficient (C_{RR}) for the vehicle can be assumed. This rolling resistance coefficient is defined as:

$$C_{RR} = \frac{F_{RR}}{F_z} \tag{3.6}$$

where F_z is the vertical load transferred through all wheels to the ground. For the low grade levels specified for most coast-down testing, this vertical load can be assumed equal to the vehicle weight ($W = mg$).

In the current analysis, dependence of the rolling resistance to vehicle speed has also been evaluated. As such the rolling resistance term in Equation 3.1 is modeled as

$$F_{RR} = C_{RR}\,(V)\,W \tag{3.7}$$

where the rolling resistance coefficient is a defined function of vehicle speed. Section 3.3.3 describes the rolling-resistance coefficient models used for the coast-down analysis.

Even during an un-powered coast, mechanical losses arise due to friction in the load-bearing rotational components of wheels and drive system. Bearing friction is generally neglected as it is a small contribution to resistance to motion. The differential(s) associated with the drive axle(s) are the major source of mechanical resistive forces. Some data suggests this resistive force is speed dependent and it is therefore modeled as such for the equation of motion:

$$F_{Mech} = F_{Mech}\,(V) \tag{3.8}$$

Section 3.3.2 describes the mechanical force models used for the coast-down analysis.

The grade force is calculated from the vehicle weight and the known grade of the track (see Section 2.2):

$$F_{Grade} = W\frac{dh}{ds} \tag{3.9}$$

Combining all the force definitions into the equation of motion (Equation 3.1) provides the following equation defining the vehicle's motion during a coast-down test:

$$m_e\frac{dV}{dt} = -\tfrac{1}{2}\,\rho\,U^2\,C_D\,(\psi)\;\;A - C_{RR}\,(V)\,W - F_{Mech}\,(V) - W\frac{dh}{ds} \tag{3.10}$$

Sections 3.3.4 and 3.3.5 describe two approaches to solve this coast-down equation of motion.

3.3.2 Mechanical Loss Model

In a coast-down test, the dominant source of mechanical loss is through the differential(s) of the drive axle(s). As part of its regulatory-development process, the EPA received data regarding the mechanical losses through an un-powered drive-axle differential of a modern heavy-duty tractor. The detailed data was shared in confidence with the EPA, but it allowed the EPA to provide estimates of mechanical losses during a coast-down procedure that are generally applicable to the coast-down of a Class 8 tractor-trailer combination. The data made public by the EPA are found in Table 3.2, which are intended for use specifically with the *High-Low Iteration* analysis method (Section 3.3.5).

Table 3.2: Mechanical loss estimates for coast-down analysis.

Speed range	Mechanical Loss
15-25 mph	100 N
60-70 mph	200 N

To include the mechanical loss data supplied by the EPA in a convenient form for different analysis procedures, models of the data from Table 3.2 were developed that provide the data as a function of vehicle speed. Two models for the mechanical losses have been developed and shown in Figure 3.2. The linear model is

$$F_{Mech} = 7.3V \quad [N] \tag{3.11}$$

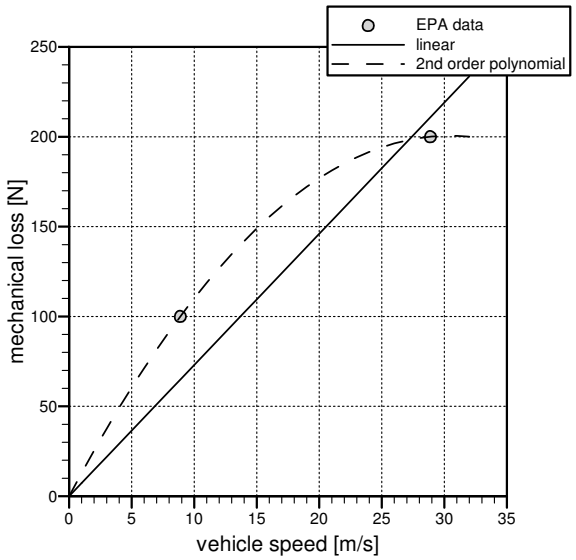

Figure 3.2: Mechanical loss models developed for coast-down analysis.

and the second-order model is

$$F_{Mech} = -0.216V^2 + 13.2V \quad [N] \tag{3.12}$$

both of which provide the mechanical loss with vehicle speed, where V is in m/s. A further linear model that intercepts both data points, without intercepting zero, is another possible option for the assumed variability of the mechanical loss with speed. Although not applied specifically in this study, a discussion surrounding its use is provided in Section 3.4.2 with the results.

3.3.3 Rolling Resistance Model

In recent years, it has come to light that the rolling resistance of heavy-duty-vehicle tires exhibit different characteristics in a coast-down environment than in a constant speed environment. A speed-dependence of the rolling-resistance coefficient has been observed in laboratory tests. The EPA had several tire sets tested by Smithers Rapra Inc. at their Ravenna Laboratory using different procedures, including a constant-speed-type procedure and a coast-down-type procedure, over a range of speeds between about 16 km/h (10 mph) and 112 km/h (70 mph). The EPA provided to NRC the data from these tests. Using a rolling-resistance model based on SAE J2452 (2008), the data has been modeled in the following form:

$$F_{RR} = P^{\alpha} L^{\beta} \left(a + bV + cV^2\right) \tag{3.13}$$

where P is the inflation pressure, L is the vertical load, V is the speed and the periphery of the tire, and α, β, a, b, and c are coefficients of the model. Using the results of the SmartWay tires tested in the coast-down test procedure, a model was developed for the ratio of the rolling resistance coefficient to its zero-speed value, as follows:

$$R_{RR} = \frac{C_{RR}}{C_{RR0}} = 1.33 \times 10^{-4} V^2 + 7.96 \times 10^{-3} V + 1.0 \tag{3.14}$$

where V is in m/s. Similarly, the tire data representing constant-speed conditions provided a variation in rolling resistance with speed but with a lower sensitivity than that for the coast-down procedure. The model developed for the constant-speed process (to be used in later parts of this report) is

$$R_{RR} = \frac{C_{RR}}{C_{RR0}} = 9.0 \times 10^{-8} V^4 + 1.0 \times 10^{-5} V^2 + 1.0 \tag{3.15}$$

These two models for the rolling-resistance are shown in Figure 3.3, from which it is evident that the rolling resistance has a much greater speed dependence under coast-down conditions that under constant-speed conditions. At 112 km/h (31 m/s) the rolling resistance is approximately 40% higher than its zero-speed value under coast-down conditions, but only 10% higher for constant-speed conditions.

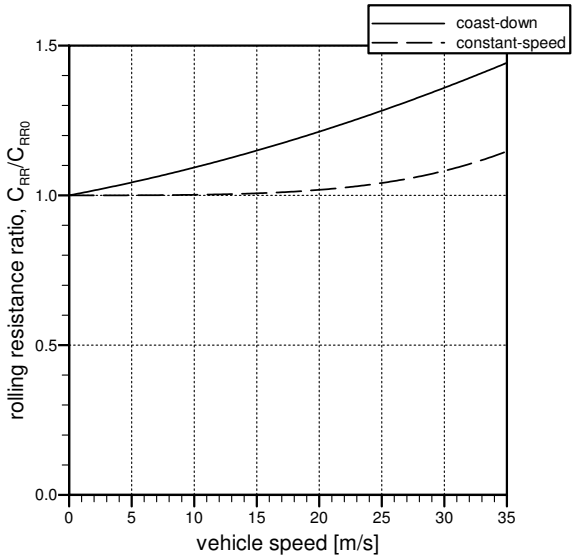

Figure 3.3: Rolling resistance models for speed dependence.

3.3.4 Analysis Using the Regression Method

The initial analysis method for GHG Phase 1 consisted of a simplified form of the SAE J1263 and J2263 coast-down procedures developed for light-duty vehicles. The J2263 method is a multi-variable regression technique that solves for the drag coefficient and the rolling resistance coefficient, and accounts for wind effects including yaw. The EPA GHG Phase 1 method (U.S. Environmental Protection Agency and U.S. Department of Transportation, 2011) neglected wind effects and mechanical resistance and assumed that the rolling resistance coefficient is constant, providing a simple regression based on a single independent variable (vehicle speed, V). A more general regression technique for Equation 3.10, that accounts for wind effects and other speed-dependent resistances, has been implemented as one of two coast-down analysis methods in the current project.

In the SAE J1263 method, the influence of wind yaw angle on the drag coefficient is introduced using a sine-squared term, as follows:

$$C_D = C_{D0} + k \sin^2(\psi) \tag{3.16}$$

Introducing this term into Equation 3.10, along with the speed-dependence for the rolling-resistance coefficient, gives the following

$$m_e \frac{dV}{dt} = -\tfrac{1}{2}\,\rho\,U^2\,C_{D0}A - \tfrac{1}{2}\,\rho\,U^2\,k\,A\,\sin^2(\psi) - C_{RR0}\,R_{RR}(V)\,W - F_{Mech}(V) - W\frac{dh}{ds} \tag{3.17}$$

Three unknowns are found in Equation 3.17, consisting of the drag area at zero yaw ($C_{D0}A$), the drag-area sensitivity to yaw (kA), and the zero-speed rolling-resistance coefficient (C_{RR0}). Using non-linear optimization techniques (for example, the *Solver* in MS Excel, or the *fminsearch* function in Matlab), these parameters can be solved given appropriate data from a coast-down run.

3.3.5 Analysis Using the High-Low Iteration Method

Based on feedback of the Phase 1 GHG coast-down process, the EPA have proposed an algebraically-simple approach to solving the coast-down equation of motion (Equation 3.10) while accounting for wind effects. Although the method specified by the EPA in the proposed test procedures (U.S. Environmental Protection Agency and U.S. Department of Transportation, 2015) assumes constant rolling resistance, it can be easily adapted to include speed-dependence to the rolling resistance coefficient, as included here.

The method proposed by the EPA for coast-down analysis is called the *High-Low Iteration* method which allows a simpler calculation procedure than the full regression method, and reduces the extent of data required for the analysis. The Phase 1 method required data measured during a full coast-down from 112 km/h (70 mph) to a full stop of the vehicle. The High-Low Iteration method only requires data for two speed ranges; a high-speed range of 112-96 km/h (70-60 mph) and a low-speed range of 40-24 km/h (25-15 mph). These reduced speed-ranges, which are not required to be part of the same coast-down run, extend the options available for test sites such as shorter test tracks that have good-quality road surfaces and well-characterized grade profiles.

The main assumption of the High-Low Iteration method is that there is a balance of net forces over each specified speed range. Using finite difference approximations to calculate the vehicle deceleration and grade loads, and using averaged wind, rolling-resistance, and mechanical-loss values over the speed range, the equation of motion is applied in the following manner:

$$m_e \frac{\Delta V}{\Delta t} = -\tfrac{1}{2}\,\rho\, U_{avg}^2\, C_D A - C_{RR0}\, R_{RR}\left(V_{avg}\right) W - F_{Mech}\left(V_{avg}\right) - W\frac{\Delta h}{\Delta s} \tag{3.18}$$

where Δ refers to the change over the speed range of the given parameter, and neglects the variability of the parameter within the speed range. Here, it is assumed that a single value of the drag coefficient is defined for the vehicle, and that the rolling-resistance coefficient can be defined by its zero-speed value (C_{RR0}) and its speed-dependent component (R_{RR}) per Section 3.3.3. It is also assumed that the mechanical force is known for each speed range (see Section 3.3.2). Rearranging the equation to isolate the unknown terms ($C_D A$ and C_{RR0}) on the left-hand side gives:

$$\tfrac{1}{2}\,\rho\, U_{avg}^2\, C_D A + C_{RR0}\, R_{RR}\left(V_{avg}\right) W = -F_{Mech}\left(V_{avg}\right) - W\frac{\Delta h}{\Delta s} - m_e \frac{\Delta V}{\Delta t} \tag{3.19}$$

With Equation 3.19 written for each speed range (high and low), this set of two equations with two unknowns can be easily solved. The direct solution of the high-speed and low-speed forms of Equation 3.19 provides an algebraic solution for $C_D A$ and C_{RR0} (solution equations not shown here). The EPA suggest an iteration method whereby assumptions of the relationships between the low-speed and high-speed values of the aerodynamic force provide a link between the two equations (U.S. Environmental Protection Agency and U.S. Department of Transportation, 2015). For six iterations, the iterative method converges to within 0.01% of the algebraic solution for $C_D A$ and 0.03% for C_{RR0}.

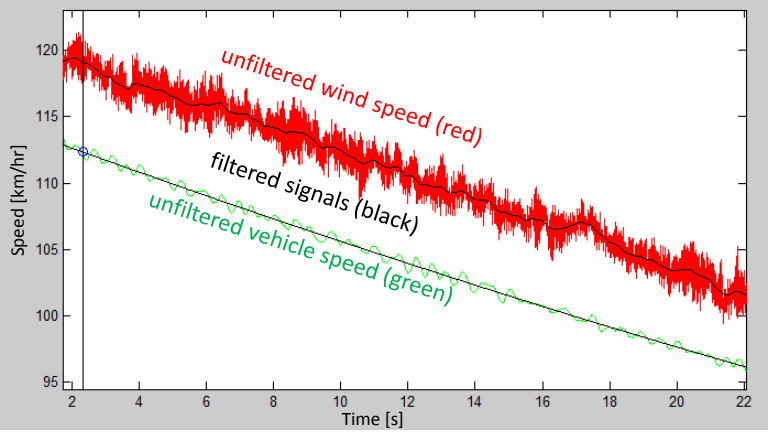

Figure 3.4: Sample vehicle and wind speed signals from a coast-down run.

3.3.6 Data Preparation

As outlined in Section 2.3, vehicle and wind data were acquired at 100 Hz and 2000 Hz, respectively. Preparation of the acquired signals was required to ensure the results of the coast-down analysis represent adequately the physics of the problem.

Upon inspection of the acquired GPS vehicle-speed data, an apparent vibration of the high-speed GPS system shows not only deceleration of the vehicle but periodic accelerations. A sample of this is shown in Figure 3.4, in which the green vehicle-speed signal shows these vibrations. The vibrations of the vehicle and its systems have been linked to the bumpiness of the track due to its aging surface quality. A 0.1 Hz low-pass filter was required to ensure no component of the vibrations infiltrated the important deceleration data required for the coast-down analysis, and in particular for the regression analysis that requires the instantaneous deceleration data. Although the High-Low Iteration Analysis is less susceptible to these non-physical vibrations, because it calculates the net deceleration over a large period of time, the vibrations in the signals must still be filtered-out. The data in Figure 3.4 shows peak-to-peak variations in the vehicle-speed data, due to the vibrations, on the order of 1 km/h. The accelerations for the High-Low Iteration analysis are based on speed ranges of 16 km/h (10 mph), and therefore an error on the deceleration calculation due to the vibrations can be up to 1/16 = 6% if the acquired signals are used without any conditioning.

Figure 3.4 also shows a sample of the wind speed data from the Cobra probe. This data has been processed and a large component of the signal is the turbulence in the wind. Some small vibrations have been identified in the Cobra probe signals due, it is assumed, to an excitation in the lateral vibration of the probe mount. When considering the frequency content of the wind signals important for a coast-down analysis, the aerodynamic admittance of the vehicle drag is expected to be negligible for small-scale/high-frequency turbulence. It is anticipated that wind gusts or turbulence on the order of the size of the vehicle and larger will have a measurable influence on the vehicle acceleration. For a 25 m long vehicle traveling at 25 m/s (90 km/h), this would mean that frequencies no higher than about 1 Hz would be expected to influence the vehicle drag. For the High-Low Iteration method, the wind-speed and wind-

angle measurements were digitally low-pass filtered with a cut-off frequency of 1 Hz, the result of which is shown in Figure 3.4.

For the Regression method, it must also be considered that the process of filtering the vehicle speed data at 0.1 Hz due to the vibrations limits the ability of the method to capture the influence of wind-gusts or changes in wind speed/angle during the coast. For the regression analysis, the wind speed was also low-pass filtered with a 0.1 Hz cut-off frequency to prevent a mismatch in signal content that might result in erroneous results. This is important particularly for the yaw-angle-sensitivity term (kA) of Equation 3.17. To evaluate the ability of the filtered data to capture wind gust effects, the coast-down data set was processed using the Regression method with and without the yaw-angle-sensitivity term. A comparison of the data sets shows inconsistent results for the kA parameter, but no significant influence of its inclusion on the solution for $C_{D0}A$. As such, the results presented in this report for the Regression method *do not* consider the wind-angle sensitivity term.

3.4 Results

The main purpose of this test program and report is to provide a verification of the coast-down testing and analysis methodology being proposed by the EPA for Phase 2 GHG regulations (U.S. Environmental Protection Agency and U.S. Department of Transportation, 2015) using a different test site. As such, most of the results presented herein are based on the EPA's proposed High-Low Iteration Method. The Regression method results are presented as a reference to the EPA proposed method. It should be noted, however, that studies of the mechanical-loss and rolling-resistance models were performed with both analysis methods, and both yielded the same trends, if not the same results for their influence.

3.4.1 EPA-Proposed High-Low Iteration Method

The coast-down measurements for the three vehicle configurations were processed using the High-Low Iteration method proposed by the EPA (U.S. Environmental Protection Agency and U.S. Department of Transportation, 2015). This version uses a 112-96 km/h (70-60 mph) high-speed range and a 40-24 km/h (25-15 mph) low-speed range for processing the data. The drag-area (C_DA) results results for each run are shown in Figure 3.5 along with running averages and standard errors calculated for each vehicle configuration (running average is represented by solid lines).

Despite the differences in individual C_DA values (± 0.4 m^2 from the mean), the running averages do not change significantly beyond 10 coast-down runs. The standard-error for the Baseline and Skirts configurations are below 1% after 10 runs, with the Skirts+Tail configuration showing a final value of 1.3% after 18 runs. The running-average and standard-error results of Figure 3.5 represent the use of all measurement runs, including those that exceed the SAE wind limits. Those with exceeded wind limits are shown as colour-filled symbols, and it it evident that these runs are some of the largest outliers from the mean. However, when

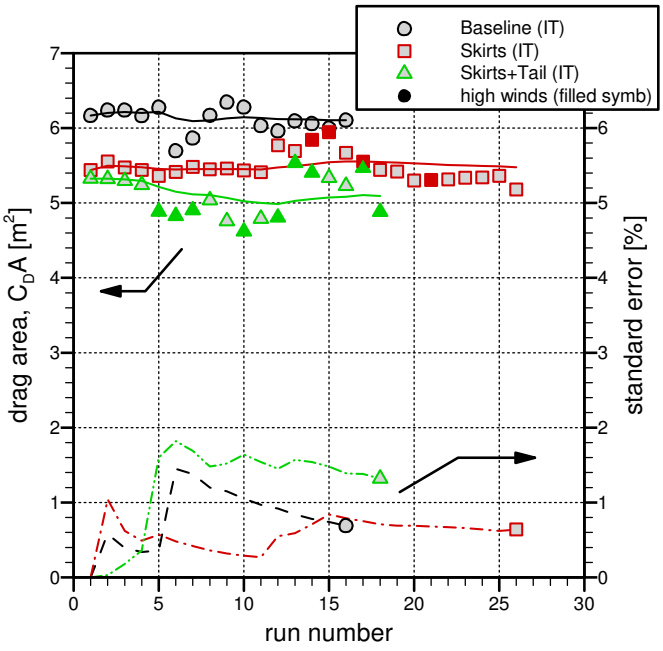

Figure 3.5: Coast-down results for C_DA using the proposed High-Low Iteration method (solid lines represent running average).

Table 3.3: Comparison of mean C_DA results of current test program with the EPA data.

Configuration	NRC (all runs) C_DA [m^2]	NRC (low-wind runs) C_DA [m^2]	EPA (runs <3°yaw) C_DA [m^2]
Baseline	6.11	6.11	5.91
Skirts	4.58	5.44	5.44
Skirts+Tail	5.09	5.15	4.89

disregarding the high-wind runs, the mean results remain within 1% of those calculated with the full data set, as shown in Table 3.3.

A comparison of the drag-area results from the current test program with those commissioned by the EPA through SwRI (data provided by the EPA) is shown in Table 3.3. The EPA data represents an average of the measurement data for which yaw angles were within ±3°for the high-speed data segments. Due to the track-oriented directionality of the winds at the test site, the NRC data set shows measurements for the high-speed data segment constrained to within +3.5° and -1.5°, as shown in Figure 3.6. The comparison of the NRC data to the EPA data in Table 3.3 is reasonable, with a difference no greater than 0.26 m^2 (5%). The yaw-distribution C_DA data of Figure 3.6 also provides some insight on the scatter of the data. From

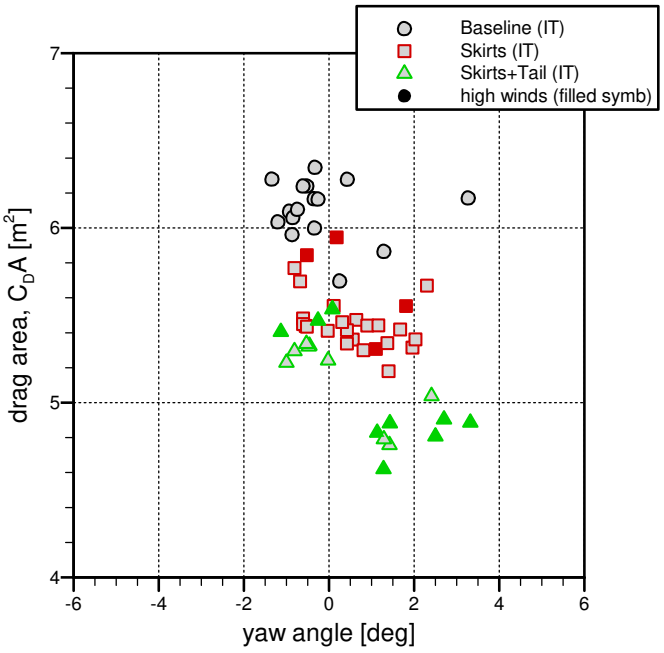

Figure 3.6: Coast-down results for $C_D A$ with yaw angle angle using the proposed High-Low Iteration method.

the Skirts+Tail data, there is a distinct shift in data between the positive and negative yaw angles. This, as will be discussed later in Section 5.2, is assumed to be a result of challenges using a high-mounted on-board wind measurement.

3.4.2 Influence of Mechanical-Loss Model

As described in Section 3.3.2, different models were developed for the mechanical resistance associated with the drive axle differential. Using the proposed EPA High-Low Iteration method, the influence of using a mechanical loss model and the sensitivity of its fidelity were investigated.

Figure 3.7 shows the changes in the mean $C_D A$ values for three levels of modeling. The 2^{nd}-order model provides the 100 N and 200 N high- and low-speed values defined in the EPA proposed method. Figure 3.7 shows that the inclusion of the mechanical loss model reduces the resultant drag-area by about 0.2 m^2 (5% reduction from red to green bars). Using the linear model provides lower $C_D A$ values. This results from the linear model over-predicting the mechanical loss for the high-speed range. Although not applied in the analysis here, the use of a linear model that intercepts the EPA-supplied data points, while not intercepting zero loss at zero speed, is another option, as described earlier in Section 3.3.2. Such a model would provide a similar magnitude of the mechanical loss component as those used for the results of Figure 3.7, and would therefore not provide a significant difference in the $C_D A$ results presented.

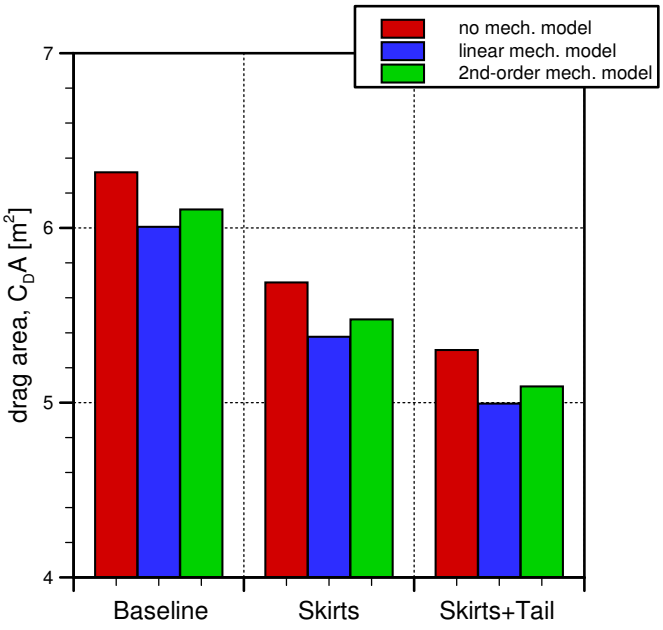

Figure 3.7: Coast-down results for C_DA using different mechanical loss models with the proposed High-Low Iteration method.

For lack of additional information on the mechanical losses at different speeds, the 2^{nd}-order mechanical-loss model has been selected for use with both the High-Low Iteration and the Regression coast-down-analysis methods.

3.4.3 Influence of Low-Speed Range for High-Low Iteration Method

As requested by the EPA, the current project has evaluated the possibility of changes to the low-speed range for the High-Low Iteration method from 40-24 km/h (25-15 mph) to 24-8 km/h (15-5 mph). The EPA has not provided mechanical-loss information for this lower speed range, however some checks were performed to verify that the mechanical loss model does not influence the evaluation of the low-speed range, and the results presented here make use of the 2^{nd}-order mechanical-loss model of Section 3.3.2.

Figure 3.8 shows the resultant C_DA values for the three vehicle configurations using the two low-speed ranges. Reducing the low-speed range is shown to increase the C_DA results on the order of 0.1 to 0.2 m^2. This increase in C_DA occurs as a result of a trade-off of the road load break-down between the aerodynamic and rolling-resistance components. Although not shown here, the resultant rolling-resistance coefficient is 10% lower using the 24-8 km/h (15-5 mph) low-speed range, as would be expected for a higher C_DA.

The reason as to why the analysis method is sensitive to this low-speed range, despite the method attempting to account adequately for the contributions of aerodynamic and rolling-

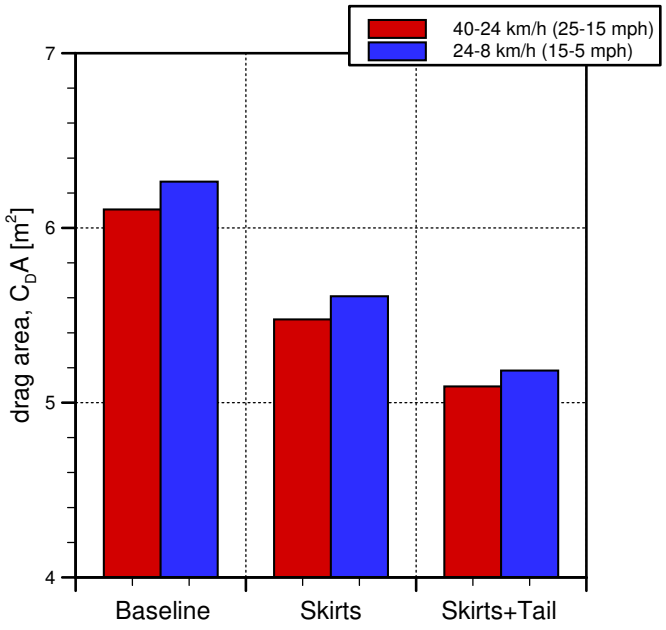

Figure 3.8: Coast-down results for C_DA using different low-speed data ranges with the proposed High-Low Iteration method.

resistance components for each speed range, is likely the accumulation of small inaccuracies associated with assumptions of the method. For example, the "net" road-load calculated for each speed range is based on a first-order/linear assumption for the non-linear change in road-load over the range. This introduces a small error in the road-load for the time period associated with each speed range. In addition, the wind speed is averaged over the same period of time, which provides a low estimate of the wind speed that should be associated with the calculated road load. Furthermore, the non-linear nature of the vehicle deceleration process means that the magnitude of these inaccuracies is different for the high- and low-speed ranges. The assumptions used to develop Equation 3.19 from Equation 3.10 are strictly valid only in the limit as the time interval Δt approach zero. The smaller change in speed, and thus road load, for the lower low-speed range introduces smaller errors in the approximations, resulting a higher level of accuracy for the method.

An additional factor that affects the influence of the low-speed range is the change in C_DA of the vehicle under the low-speed conditions. Reynolds number effects lead to changes in C_DA at low speeds, and the much higher yaw angles that are often experienced at these low speeds (can exceed 30°) also contribute to higher C_DA values (up to 50% higher for modern tractor-trailer combinations). The High-Low Iteration method and the Regression method implemented for this analysis assume a constant C_DA value for the vehicle over its entire speed range. Minimizing the aerodynamic component of the road load in the low-speed range, accomplished by using lower speeds, reduces the errors associated with the constant-C_DA assumption. It is therefore recommended to use the lowest low-speed range possible to minimize the aerodynamic force and reduce these errors.

3.4.4 Influence of Rolling-Resistance Model

As described in Section 3.3.3, the rolling-resistance of heavy-duty-vehicle tires has been shown in recent years to exhibit different characteristics in a coast-down environment than in a constant speed environment. To date, coast-down analyses have typically considered the rolling resistance to be constant during a vehicle coast-down test. This assumption is evaluated using the current data set by applying the High-Low Iteration method assuming a constant rolling-resistance coefficient and assuming the speed-dependent model of Equation 3.14. Figure 3.9 shows the results of the comparison, from which it is evident that accounting for the rolling-resistance variation with speed results in $C_D A$ values on the order of 0.4 to 0.5 m^2 lower (order of 10% lower). This occurs due to a higher component of rolling resistance present in the road load at higher speeds. The use of a speed-dependent C_{RR} also influences the C_{RR0} value calculated by the method, with a decrease on the order of 3% (not shown). It is recommended to use the speed-variable rolling-resistance model with any future coast-down analysis.

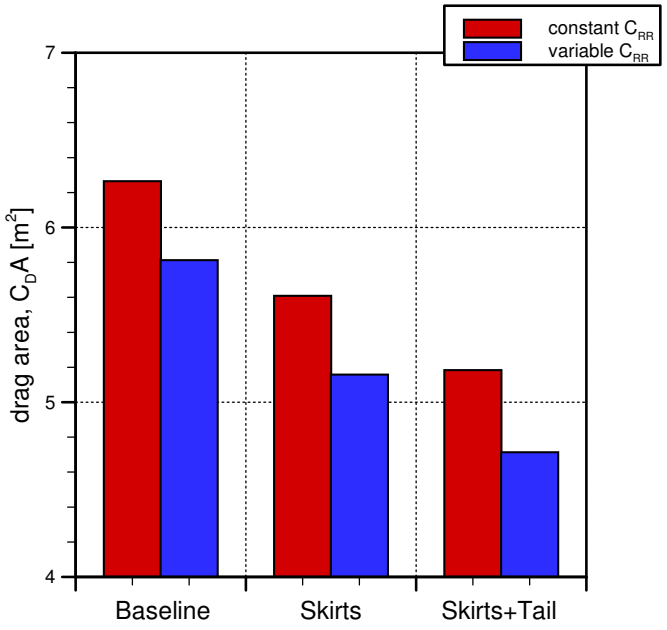

Figure 3.9: Coast-down results for $C_D A$ using constant and speed-dependent rolling-resistance models with the proposed High-Low Iteration method.

3.4.5 Regression Method

The regression method described in Section 3.3.4 has been used to solve for the drag area ($C_D A$) and zero-speed rolling-resistance coefficient (C_{RR0}) values of the current data set using the 2^{nd}-order mechanical loss model and the speed-dependent rolling-resistance-coefficient model. The results are shown in Figure 3.10 contrasted with the equivalent results from the High-Low Iteration method. The running averages for each method are represented by solid and dashed lines, which are nearly indistinguishable from each other, despite a difference in the individual $C_D A$ values. As a result, both methods give similar mean $C_D A$ values even though there are some differences in the $C_D A$ values calculated for each individual run. Both methods provide standard errors at or below about 1%.

The drag-area data for the two methods are shown plotted against yaw angle in Figure 3.11. The yaw angle identified for the Regression data set represents the average yaw angle over the high-speed measurement run, which has its highest speed at about 112 km/hr (70 mph) as with the High-Low Iteration method, but with a low speed near about 65 km/h (40 mph). Higher yaw angles observed over this greater speed range introduce higher averaged yaw angles associated with the Regression data set.

Excellent agreement in mean $C_{D0} A$ values between the two methods is observed, as tabulated in Table 3.4, with a difference no greater than 0.01 m^2 (0.2%). This adds confidence that the EPA-proposed High-Low Iteration method is appropriate for vehicle-drag measurements and

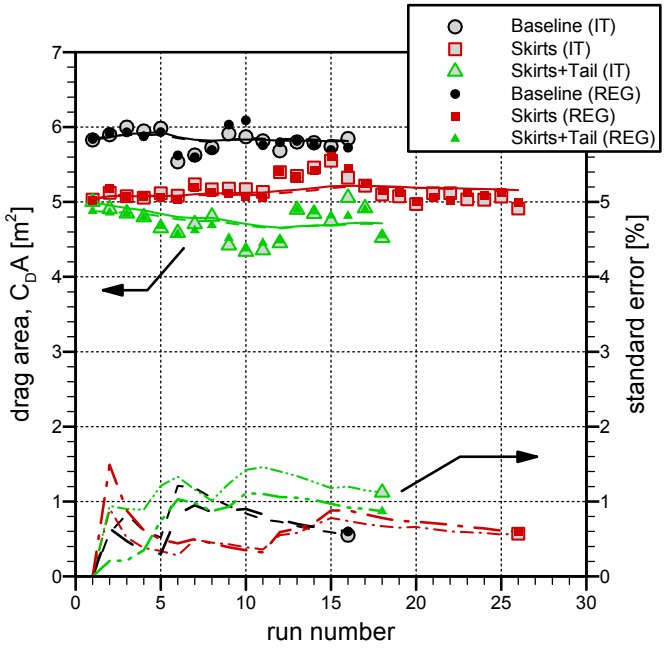

Figure 3.10: Coast-down results for $C_D A$ using the Regression and the High-Low Iteration methods (solid/dashed lines represent running average for the iteration and regression methods, respectively).

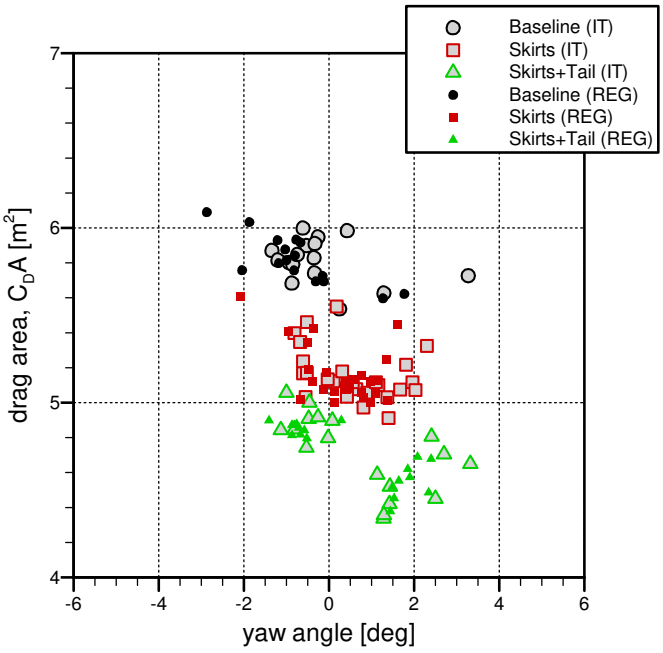

Figure 3.11: Coast-down results for C_DA with yaw angle using the Regression and the High-Low Iteration methods (solid/dashed lines represent running average).

Table 3.4: Comparison of mean C_DA and C_{RR0} results for the High-Low Iteration method and the Regression method.

Configuration	**Drag Area C_DA [m^2]**		**Rolling Resistance Coeff. C_{RR0} [-]**	
	Iteration	**Regression**	**Iteration**	**Regression**
Baseline	5.81	5.82	0.0049	0.0050
Skirts	5.16	5.16	0.0049	0.0050
Skirts+Tail	4.71	4.70	0.0053	0.0053

captures the important physics of the problem, despite its simplifying assumptions.

The rolling-resistance-coefficient results calculated using both methods are presented in Figure 3.12 and also tabulated in Table 3.4. The results in Figure 3.12 show a greater run-to-run variability for C_{RR} than was observed for C_DA,but good agreement between the averaged values of the two methods has been found (2% difference).

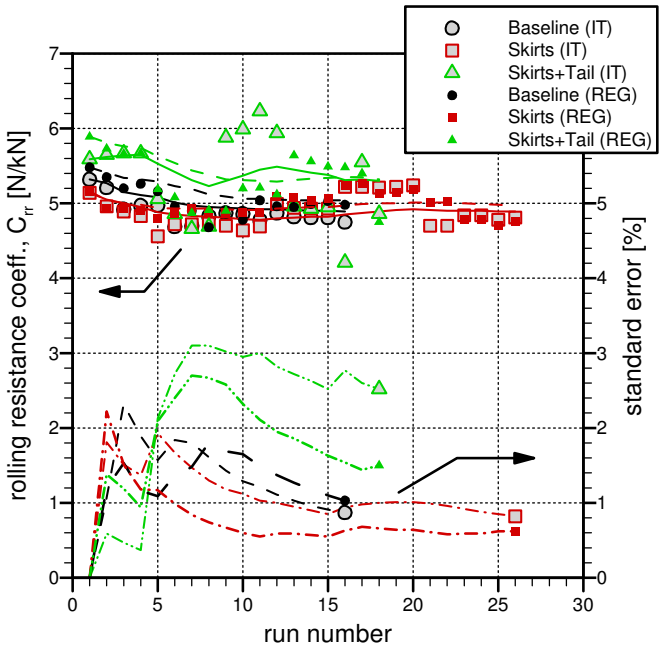

Figure 3.12: Coast-down results for C_{RR0} using the Regression and the High-Low Iteration methods (solid/dashed lines represent running average).

4. Constant-Speed Method

4.1 Test Procedures

The constant-speed tests were performed on the "Bravo" track at the Motor Vehicle Test Centre operated by PMG Technologies in Blainvile, Québec. The tests were performed with the vehicle and instrumentation as described in Section 2. Pre-run inspections and checks were conducted to ensure that the vehicle condition was consistent from test to test. Specific items checked included:

1. Cold tire inflation pressure;
2. Doors and windows were fully closed;
3. HVAC and A/C settings remained consistent; and
4. Fuel level at least 3/4 full.

Prior to the start of testing, the vehicle was warmed up by driving normally for several laps of the track. During this time, the track-side instrumentation was initialized and checked.

Standards or recommended practices for constant-speed testing of heavy-duty vehicles do not exist. The general procedure to be followed for this is based on specifications proposed by the EPA in 2015 (U.S. Environmental Protection Agency and U.S. Department of Transportation, 2015.

The vehicle was operated at each speed for approximately 90 minutes of steady-state cruise (see Section 4.2 for test conditions). Prior to the start of, and immediately at the conclusion of each constant speed test run, the tire pressure was recorded and the Cobra Probe zeroed.

The test procedures used for the constant-speed tests were as follows:

1. The data acquisition system was started. The Cobra Probe zeroed.
2. The vehicle was accelerated to the desired test speed, based on the GPS speed readout. The vehicle's cruise control was then used to assist in maintaining constant speed.
3. The driver attempted to maintain as constant a speed as possible, even when negotiating the turns at each end of Bravo. The Bravo turns are banked and the driver was free to use the banked turns to minimize cornering effort.
4. As the vehicle entered the straight section of Bravo, the travel direction was straightened. Regardless of travel direction, the test vehicle maintained the "outside" position on the straight section of Bravo track.
5. After 90 minutes were completed, the vehicle was stopped, the data acquisition system was halted, and the recorded data was saved.
6. The running direction was reversed and steps 1 through 5 inclusive were repeated.

Both the north and south sides of the Bravo track were used for the constant-speed tests.

4.2 Test Conditions

The track consists of 1.6 km straight sections used for the constant-speed runs. Three test speeds were defined for the constant-speed test program:

- High-Speed: 112 km/h (70 mph)
- Medium-Speed: 80 km/h (50 mph)
- Low-Speed: 16 km/h (10 mph)

For each measurement run, the vehicle was driven at constant speed around the track in either the clockwise or counter-clockwise orientation, with data collected during the entire duration. During post-processing of the data, only constant-speed segments over the straight sections of the track were used, adjusted to avoid a settling period of the cruise control entering the straight sections. As described in Section 2.2, the south-side of the track consists of two sections of nearly-equal but opposite grade levels, with a peak near the middle. The vehicle cruise-control system required time to adjust to the new grade as the vehicle passed over the peak. This settling period was also removed from the processed data.

For each vehicle configuration, a target of 90 minutes per constant speed run was specified. Of this period, approximately 1/3 was found to provide data appropriate for a constant-speed analysis. Table 4.1 lists the total duration of usable constant-speed data acquired for each of the three vehicle configurations. More data were acquired for the Skirts configuration at 80 km/h in an attempt capture a greater range of wind conditions.

Table 4.1: Test matrix for constant-speed runs (CW - clockwise direction, CCW - counter-clockwise direction).

	16 km/h (10 mph)		**80 km/h (50 mph)**		**112 km/h (70 mph)**	
	CCW	**CW**	**CCW**	**CW**	**CCW**	**CW**
Baseline	30 min	-	30 min	30 min	20 min	30 min
Skirts	30 min	30 min	75 min	60 min	30 min	30 min
Skirts+Tail	30 min	30 min	-	30 min	30 min	30 min

4.3 Constant-Speed Analysis

4.3.1 Equation of Motion

The concept of constant-speed analysis is to infer the external forces acting on a vehicle based on the power required to maintain the vehicle at constant speed. Figure 3.1 shows a pseudo free-body diagram of a vehicle travelling at constant speed. The forces that impact forward motion to the vehicle are:

- Aerodynamic Drag (F_{Aero}) - resistive force as the vehicle moves through the air;
- Rolling Resistance (F_{RR}) - resistive force due to deformation of the tire material at the interface with the ground;
- Grade Force (F_{Grade}) - component of the vehicle weight in the direction of motion due to the grade/inclination of the road surface from horizontal, and
- Tractive Force (F_{Trac}) - Force delivered by the driven wheels to maintain speed.

The aerodynamic drag, rolling resistance and grade force contribute to the Road Load (F_{RL}), which is the combination of external forces acting on the vehicle while in motion.

Applying Newton's 2^{nd} law of motion in the direction of motion of the vehicle, the resulting equation is

$$m_e \frac{dV}{dt} = F_{Trac} - F_{Aero} - F_{RR} - F_{Grade} \tag{4.1}$$

for which m_e is the effective mass (see Section 3.3.1). The EPA-proposed constant-speed analysis method assumes that the vehicle is maintained at a constant speed at all times, and therefore the vehicle's acceleration is zero and the left side of Equation 4.1 is set to zero. This introduces an approximation that may not be valid under all conditions.

The aerodynamic drag force is the parameter of most interest for the current investigation. As in Section 3.3.1 for the coast-down method, the drag force for a vehicle can be defined as

$$F_{Aero} = Q\, C_D\,(\psi)\;\; A \tag{4.2}$$

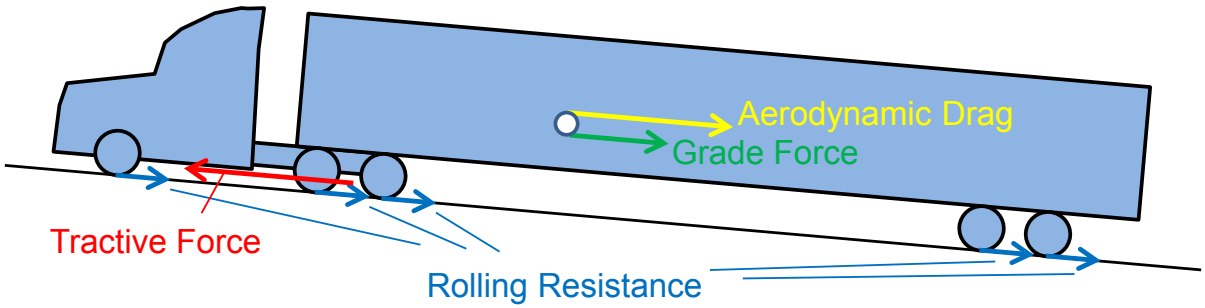

Figure 4.1: Free-body diagram of a vehicle at constant speed.

where the dynamic pressure of the wind (Q) is dependent on the air density (ρ) and wind speed relative to the vehicle (U):

$$Q = \tfrac{1}{2}\,\rho\,U^2 \tag{4.3}$$

The rolling resistance (F_{RR}) of a tire can be affected by many factors such as vertical load on the tire, inflation pressure, rotational speed, and ground texture. In conventional coast-down testing, such as the SAE J1263 and J2263 procedures, it is assumed that only vertical load influences the rolling resistance, and that all tires on the vehicle behave in the same manner such that a constant rolling-resistance coefficient (C_{RR}) for the vehicle can be assumed. This rolling resistance coefficient is defined as:

$$C_{RR} = \frac{F_{RR}}{F_z} \tag{4.4}$$

where F_z is the vertical load transferred through all wheels to the ground. For the low grade levels defined for most coast-down testing, this vertical load can be assumed equal to the vehicle weight ($F_z \approx W = mg$).

Section 3.3.3 described the rolling-resistance variation with speed for coast-down and constant-speed test methodologies. The rolling-resistance force is therefore modeled as

$$F_{RR} = C_{RR}\,(V)\,W \tag{4.5}$$

where the rolling resistance coefficient is a defined function of vehicle speed.

The grade force is calculated from the vehicle weight and the known grade of the track (see Section 2.2):

$$F_{Grade} = W\frac{dh}{ds} \tag{4.6}$$

The tractive force required to maintain the vehicle's speed has been measured using a drive-shaft torque meter (τ_{shaft}), installed on the drive-shaft between the transmission and the differential. Using the measurement of shaft rotational speed (ω_{shaft}), the tractive force delivered to the ground is

$$F_{Trac} = \frac{\tau_{shaft}\,\omega_{shaft}\,\eta}{V} \tag{4.7}$$

where V is the vehicle speed. Unlike the coast-down analysis that required a specification for the mechanical loss across the differential, the constant-speed analysis used here accounts for these losses through a efficiency factor (η) applied to the shaft power. Based on constant-speed measurements performed by SwRI for the ECCC Pro-Star tractor, during which the drive-shaft torque measurements were performed in parallel with wheel-torque measurements, the efficiency factor used for the current test is η = 93.2%.

Combining all the force definitions into the equation of motion (Equation 4.1) provides the following equation defining the vehicle's motion during a constant-speed test:

$$Q\,C_D\,(\psi)\;\;A + C_{RR0}\,R_{RR}\,(V)\,W = \frac{\tau_{shaft}\,\omega_{shaft}}{V\,\eta} - W\frac{dh}{ds} \tag{4.8}$$

Two options are available to solve this equation for the drag-area (C_DA) and rolling-resistance (C_{RR0}) as described in the next section.

4.3.2 Solution Methods

Two approaches can be used to solve the constant-speed equation of motion (Equation 4.8) using the data measured during the test program. In an attempt to capture transient effects during the test, such as changes in wind-speed and yaw angle, the time-series of constant-speed data are averaged over specific time intervals. Based on an initial assessment of adequate convergence of such averages, 30 s averaging has been performed for the 16 km/h (10 mph) data and 20 s averaging has been performed for the 80 km/h (50 mph) and 112 km/h (70 mph) data. The road load for each data point (index i) has been calculated as

$$F_{RLi} = \overline{\left[\frac{\tau_{shaft}(t)\ \omega_{shaft}}{V\ \eta} - W\frac{dh}{ds}\right]} \tag{4.9}$$

where the over-bar denotes an average over the 20 s or 30 s period. This averaging process reduces the sensitivity of the calculation to grade effects, and therefore the low-resolution grade survey for both sides of the track were found to be sufficient for the calculation of Equation 4.9.

The first method to solve Equation 4.8, in a manner proposed by the EPA, is to assume that the road load measurements at 16 km/h (10 mph) are comprised solely of rolling resistance and grade loads (no aerodynamic loads), such that the rolling-resistance coefficient is calculated as

$$C_{RR0i} = \frac{F_{RLi}}{R_{RR}\,(V_i)\,W_i} \tag{4.10}$$

for each 30 s-averaged data point (index i). According to Equation 3.15 in Section 3.3.3, the sensitivity of rolling resistance to vehicle speed at 16 km/h is negligible ($R_{RR}\,(16\,km/h) = 1.0002 \approx 1$) and therefore is not strictly required in the calculation of C_{RR0}. For a given vehicle configuration, the net rolling-resistance coefficient C_{RR0} is calculated as the average of all measured points:

$$\overline{C_{RR0}} = \frac{1}{N}\sum_{i=1}^{N} C_{RR0i} \tag{4.11}$$

The next step is to use $\overline{C_{RR0}}$ to calculate and subtract the rolling resistance for each F_{RLi} value measured at 80 km/h (50 mph) and 112 km/h (70 mph):

$$C_D A_i = \frac{F_{RLi} - \overline{C_{RR0}}\ R_{RR}\,(V_i)\,W_i}{Q_i} \tag{4.12}$$

Each $C_D A_i$ value is then associated with a yaw angle ψ_i averaged over the same 20 s time interval. This method is called the *Subtraction* method for the remainder of this report.

The second solution approach to Equation 4.8 is to apply a regression technique using all individual F_{RLi} data points. This is equivalent to the approach taken for the coast-down regression analysis (Section 3.3.4), whereby each road-load data point is derived from a segment of a constant-speed test, rather than an instant of a coast-down run. The higher yaw-angle range associated with the constant-speed measurements also allows the inclusion of the yaw-sensitivity parameter kA introduced in Equation 3.17 in Section 3.3.4. This method will be called the *Regression* method for the remainder of this report.

The European Commission (EC) has proposed constant-speed testing as its reference method for greenhouse-gas emissions regulations. The proposed EC method, as most recently documented by (Fontaras *et al.*, 2014), requires data at two speeds, from which a regression technique is used to extract $C_D A$ and C_{RR}. The method assumes constant rolling resistance and therefore the regression is a quadratic fit of the road load data with wind speed, neglecting the first-order term. This is equivalent to a linear fit of road-load with dynamic pressure, from which the offset is the rolling resistance and the slope is the drag area. The method is therefore similar to the Regression method above, but does not require multi-variable regression due to the constant rolling resistance and the neglect of a yaw term in the regression analysis.

4.3.3 Data Preparation

As with the coast-down tests, vehicle and wind data were acquired at 100 Hz and 2000 Hz, respectively. Preparation of the acquired signals was required to ensure the results of the coast-down analysis represent adequately the physics of the problem. Filtering of the on-board wind data was performed with a 1 Hz cut-off frequency, as with the coast-down data.

Section 2.3 described a strong fluctuation in the drive-shaft torque measurement with a distinct frequency of about 7 Hz regardless of the vehicle speed. Figure 4.2 shows an subset of data from a low wind 112 km/h constant speed test, in which the calculated road load is presented for three laps of the track. The black line represents a direct calculation of the road load, corrected for grade, showing large instantaneous changes as a result of the 7 Hz torque fluctuations. The red line in Figure 4.2 represents the same data calculated from signals filtered at 0.5 Hz. The similarity in filtered road-load signals for each side of the track provide confidence that the filtering is effective. Of particular note is a large drop in road load on the south side passes of the track, identified by the red arrows. These drops in signal are associated with a reduction in power delivered by the engine as the vehicle begins its downhill descent due to the change in grade at mid-point of the south-side stretch. The vehicle cruise control system is slow to respond and requires a significant time/distance to recover to steady-state conditions. These settling periods have been removed from the data set.

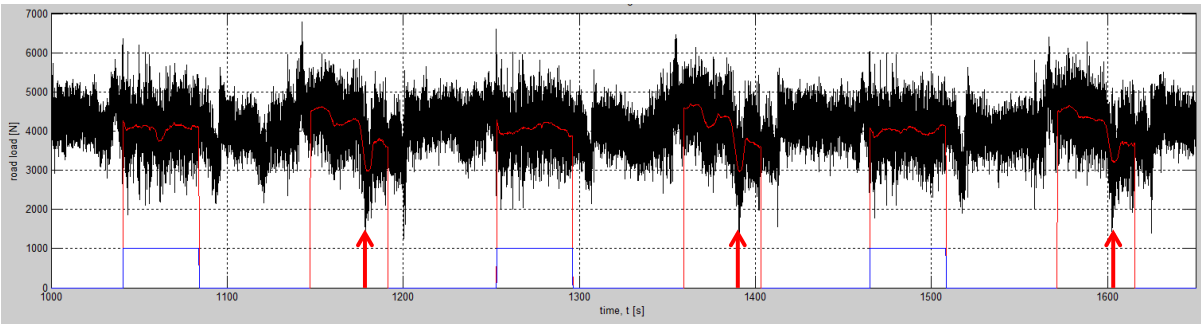

Figure 4.2: Sample vehicle road load measurement in time for a low-wind constant speed run for three laps of the track (black line - unfiltered road load, red line - filtered road load on straight sections, red arrows - identify cruise control lag on south side pass).

4.4 Results

The constant-speed data measured during the test campaign at the Motor Vehicle Test Centre in October 2015 was first analyzed using the Subtraction and the Regression methods described in the previous section. The results are shown in Figure 4.3. These results identify the ability of the constant-speed method to acquire data associated with larger yaw angles than the coast-down results of Section 4.4, but with a significant level of scatter for the Subtraction-method results, much greater than for the coast-down data. As defined, the Regression method provides a drag-area characteristics curve that characterize the variation of $C_D A$ with yaw angle. However, the yaw-variations are distinctly different for each vehicle configuration, and are not considered reliable as they have been inferred from the same scattered data set from which the Subtraction-method results have been calculated. Table 4.2 shows the results of the zero-yaw drag-area values ($C_{D0}A$) defined using both constant-speed analysis methods, with those from the Subtraction method representing an average of the data within yaw angles of $\pm 2^\circ$. A significant level of scatter was also found in the rolling-resistance-coefficient data using 30-second data segments of the 16 km/h (10 mph) data sets, with different averaged values for each vehicle configuration, as also provided in Table 4.2. The inconsistency in $C_{D0}A$ and C_{RR0} values between the two methods is in large part due to the significant scatter in the data.

A secondary Subtraction-method evaluation of the data presented in Figure 4.3 has been performed with restrictions placed on the validity of each 30 s or 20 s mean data point. Only

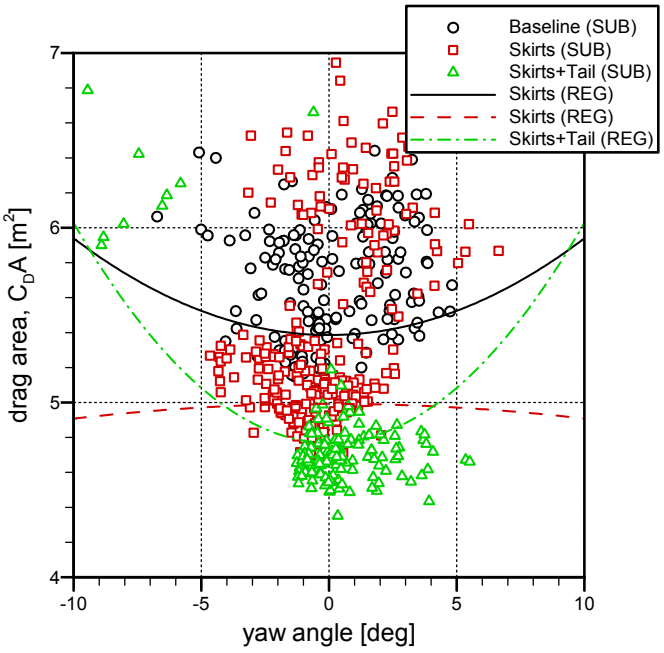

Figure 4.3: Constant-speed results for $C_D A$ with yaw angle using the Subtraction (SUB) and the Regression (REG) methods.

Table 4.2: Comparison of mean $C_{D0}A$ and C_{RR0} results for the constant-speed Subtraction method and the Regression method.

Configuration	Drag Area $C_{D0}A$ [m^2]		Rolling Resistance Coeff. C_{RR0} [-]	
	Subtraction	Regression	Subtraction	Regression
Baseline	5.65	5.38	0.0063	0.0067
Skirts	5.32	4.99	0.0057	0.0061
Skirts+Tail	4.71	4.76	0.0055	0.0052

data from the 16 km/h (10 mph) data set for which the mean winds did not exceed 5 m/s and $\pm 10^\circ$yaw were used to define the rolling-resistance coefficient. A single value of C_{RR0} = 0.0055 was then used to calculate the speed-dependent rolling resistance to be subtracted from the data for all three vehicle configurations. To eliminate the significant scatter observed in the $C_D A$ values, the following restrictions were imposed on the 80 km/h (50 mph) and 112 km/h (70 mph) data:

- the mean wind speed over the 20 s data point must be within 5% of the mean vehicle speed;
- the mean yaw-angle over the 20 s data point must be within $\pm 3^\circ$of zero yaw;
- the range of yaw angles over the 20 s data point (max-min) must be no greater than 6°; and
- the filtered road-load must not deviate more than $\pm 10\%$ from its mean value over the 20 s data point.

Applying these restriction to the data eliminated between 60% and 90% of the data points for each vehicle configuration. Applying these restrictions, the Subtraction analysis method provides the results shown in Figure 4.4. There remains scatter in the data of Figure 4.4, but clusters of $C_D A$ values for each vehicle configuration provide increased confidence that the results are representative of the drag-area of the vehicle. Table 4.3 shows the $C_{D0}A$ and C_{RR0} results from this refined analysis, with a measure of the total time period of data used to calculate the drag area values. The $C_{D0}A$ values of Table 4.3 represent an average of the data within yaw angles of $\pm 2^\circ$. The restrictions introduced to eliminate the large scatter in the data serve to reduce the available range of yaw-angle data to a similar range as observed from the coast-down results. Section 5 compares and contrasts these constant-speed results with the coast-down results.

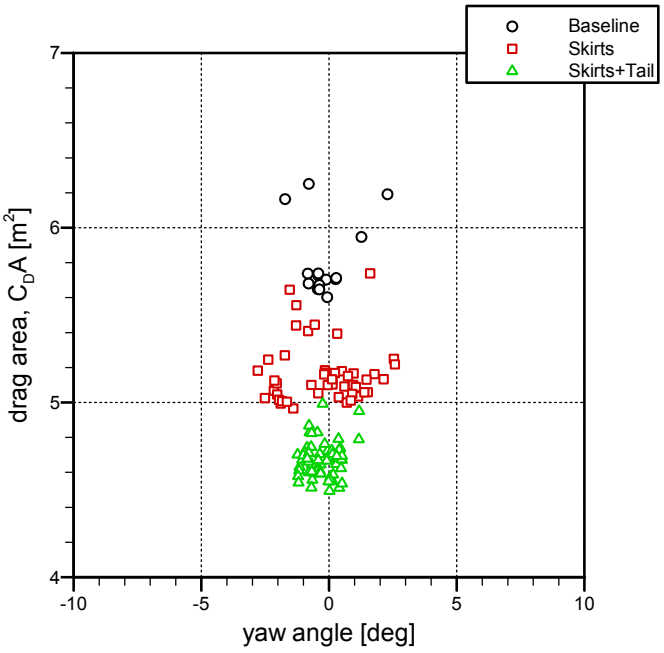

Figure 4.4: Constant-speed results for $C_D A$ with yaw angle using the Subtraction method with additional restrictions imposed on data validity.

Table 4.3: Comparison of mean $C_{D0}A$ and C_{RR0} results for the constant-speed Subtraction method with additional restrictions on data validity.

Configuration	**Drag Area** $C_{D0}A$ **[m^2]**	**Rolling Resistance Coeff.** C_{RR0} **[-]**	**Averaging Time [min]**
Baseline	5.77	0.0055	5.0
Skirts	5.17	0.0055	12.7
Skirts+Tail	4.67	0.0055	20.7

5. Comparison of Methods and Other Considerations

5.1 Comparison of Coast-down and Constant-speed Results

In the previous two major sections of this report, the coast-down and constant-speed test methodologies and results were presented. In this section the results from the high/low iteration method for coast-down testing is compared to the subtraction method for constant speed testing. The version of the coast-down iteration method applied here consists of that with the 24-8 km/h (15-5 mph) low-speed segment, making use of the second-order mechanical resistance and the speed-dependent rolling resistance models. The version of the constant-speed subtraction method consists of that with the additional restriction to minimize the level of scatter in the results.

Figure 5.1 shows a comparison of the C_DA results for the coast-down and constant-speed methods, with the zero-yaw drag area ($C_{D0}A$) values and zero-speed rolling-resistance coefficient (C_{RR0}) values tabulated in Table 5.2. Despite some of the scatter in Figure 5.1, there is reasonable agreement in the data for both methods. For each vehicle configuration, the data from the two methods cluster well, such that they could be considered as combined data sets. While the clustering adds confidence to the data, the scatter from each single run/point as representative of the mean is large, and therefore the confidence interval is large for the data set. The averaged $C_{D0}A$ values of Table 5.2 are also in good agreement, with less than 1% difference between the two methods. A greater difference is observed in the C_{RR0} data of table Table 5.2, but it is important to recognize that these methods should not be expected to provide the same values. The tire data supplied by the EPA, from which the rolling-resistance models of Section 3.3.3 were derived, shows low-speed rolling resistance tested at constant speed on the order of 10-20% higher than the equivalent values tested in a coast-down type procedure.

The agreement in results between the two testing methods provide additional confidence that the assumptions made in the analyses are reasonable and appropriate. The major drawback to the current data set is the inability to acquire quality data at higher yaw angles. This was one of the factors that led the EPA to consider a constant-speed procedure. The ability to measure data, on the road or track, at higher yaw angles could provide a means of evaluating the wind-averaged drag of a vehicle (WAC_DA) which is being considered by EPA as the C_DA input parameter for the GEM as more representative measure of the aerodynamic performance of a vehicle than the zero-yaw $C_{D0}A$ value. This data set appears to confirm that both the coast-down and the constant-speed approaches are viable means to evaluate the drag-area of a heavy-duty vehicle under low-yaw-angle conditions.

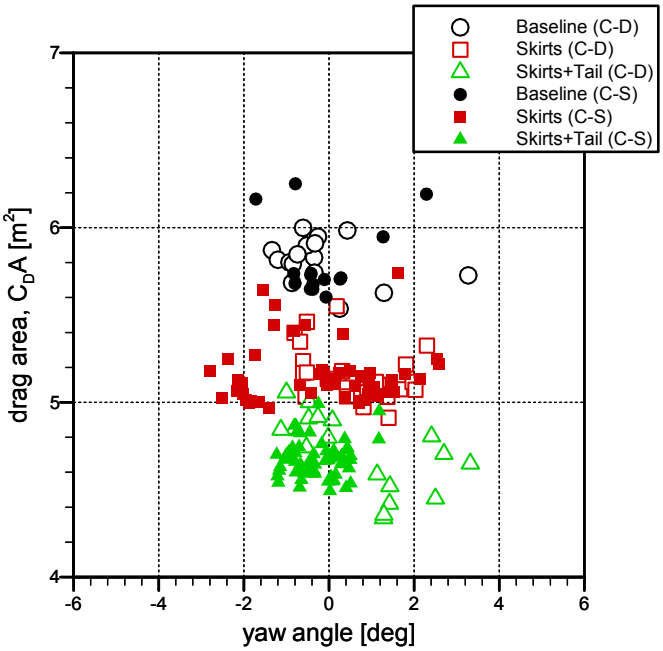

Figure 5.1: Comparison of coast-down and constant-speed results for C_DA with yaw angle for the coast-down Iteration method and the constant-speed Subtraction (with additional restrictions) method.

Figure 5.2: Comparison of mean $C_{D0}A$ and C_{RR0} results for the coast-down Iteration method and the constant-speed Subtraction (with additional restrictions) method.

Configuration	**Drag Area $C_{D0}A$ [m^2]**		**Rolling Resistance Coeff. C_{RR0} [-]**	
	Coast-Down	**Constant-Speed**	**Coast-Down**	**Constant-Speed**
Baseline	5.81	5.77	0.0050	0.0055†
Skirts	5.16	5.17	0.0050	0.0055†
Skirts+Tail	4.71	4.67	0.0053	0.0055†

† single value defined using data from all three vehicle configurations

5.2 Comments on the Influence of Wind Measurements

Discussions with the EPA at the outset of this project identified an odd trend in the results of some of the SwRI/EPA data set. Greater cross-winds were experienced in their testing and it was found that some coast-down and constant-speed data showed an asymmetry of the data about zero yaw angle. This is similar to the asymmetry observed for the coast-down "Skirts+Tail" data in Figure 5.1 for which the cluster of data around +2°yaw is much lower than the cluster of data around -1°yaw. In the EPA data set, the asymmetry is not vehicle specific, as it was observed for different vehicles, and it switched sides (about zero yaw) for testing on different days with the same vehicle, implying an environmental influence. The results from the current test campaign have provided some insight to the problem.

For the asymmetric "Skirts+Tail" coast-down data, the data cluster at positive yaw were measured with strong head winds, and the cluster at negative yaw were measured with strong tail winds. This prompted an investigation to the on-board wind measurement and the potential error associated with its calibration against the track-side anemometers. Although a linear fit between the on-board-to-track-side wind measurements was found (see Figure 2.8), the scatter in the data about the wind-speed fit is on the order of $\pm$5% which implies that other factors may influence the calibration. It should be noted that a 5% error in wind speed results in a 13% error in dynamic pressure, which thus introduces a 13% error in $C_D A$ associated with the wind measurement.

Based on some conceptual arguments surrounding the nature of terrestrial winds near the ground, and considerations of the placement of the track-side and on-board wind measurements, the likely source of yaw asymmetry is an error in the wind-speed calibration associated with the height differential between the two wind-measurement systems. This argument has been discussed previously by Cooper (1999) and is outlined in the following discussion.

The terrestrial winds near the ground change with height. A simple approximation to this change with height can be represented by a power-law profile

$$u(z) = u_{ref} \left(\frac{z}{z_{ref}} \right)^{\alpha} \tag{5.1}$$

whereby the wind speed increases with height. An exponent of $\alpha = 1/7$ is typical for defining the change in wind speed with height over open-land surfaces which, although is not strictly applicable for the forested surroundings of the track and the very near-ground region in which a vehicle operates, is useful for demonstrating the issue at hand. The important concept is the shear, or change-with-height, of the wind speed.

If it is assumed that the terrestrial winds are aligned with the motion of the vehicle (head-wind or tail-wind only), then the wind profile experienced by the vehicle is

$$U(z) = V \pm u_{ref} \left(\frac{z}{z_{ref}} \right)^{\alpha} \tag{5.2}$$

where V is the vehicle ground speed. This result shows that the wind speed experienced by the vehicle changes with height, which is dependent on the direction of the terrestrial winds

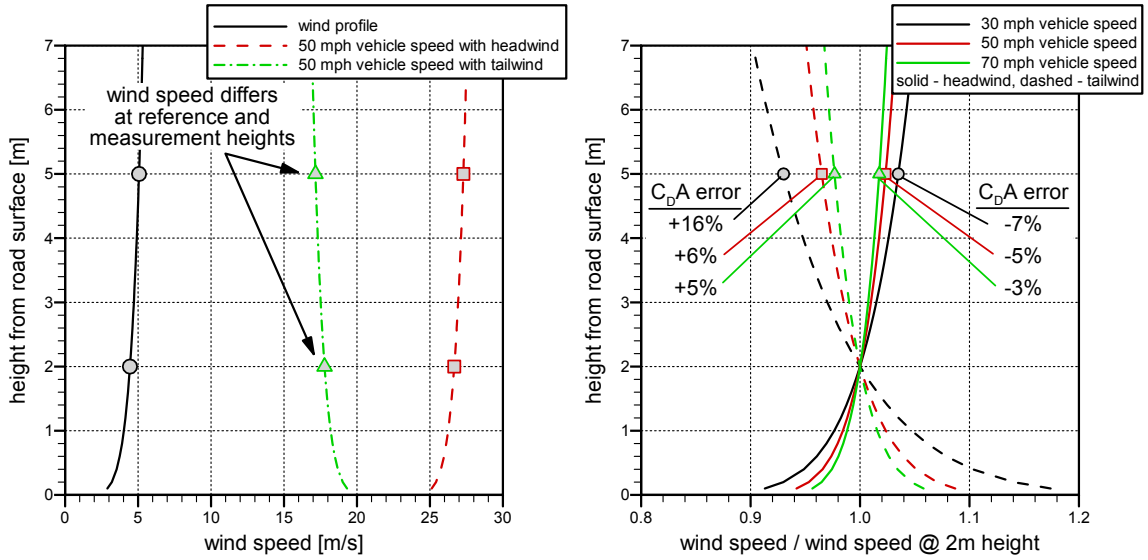

Figure 5.3: Sample wind profiles experienced by the vehicle in a 16 km/h (10 mph) head-winds or tail-wind.

relative to the vehicle motion. In considering the placement of the on-board and track-side wind measurement devices (5 m and 2 m, respectively), the calibration of the on-board device will change depending on the strength (u_{ref}) and shear (α) of the terrestrial winds. If the winds are not directly aligned with the vehicle motion, a change with height of the yaw angle is also experienced by the vehicle, however this is not discussed here for brevity.

To provide an example of the potential influence of the height differential between the track-side and on-board wind measurements, some sample wind profiles are shown in Figure 5.3 that have been calculated assuming a 16 km/h (10 mph) wind strength at 2 m height from the ground. The left plot shows the terrestrial wind profile and the wind profile experienced by a vehicle traveling at 80 km/h (50 mph) in a head-wind or tail-wind scenario. It is evident that there is a difference in wind speed at the on-board measurement height (5 m) compared to the track-side measurement height (2 m). The right plot of Figure 5.3 shows these profiles, along with those assuming 48 km/h (30 mph) and 112 km/h (70 mph) vehicle speeds, normalized by the wind speed at 2 m height. It is evident that the wind speed at 5 m height can vary significantly from the 2 m height value by at least several percent. The error introduced in calculating C_DA associated with these particular assumptions on the wind profile are also highlighted in Figure 5.3, which shows that even at high vehicle speeds, errors on C_DA in excess of 5% are possible, depending on the wind conditions. This magnitude could easily account for the spread in head-wind and tail-wind clusters of coast-down data for the "Skirts+Tail" configuration in Figure 5.1, for which strong winds were present during the tests.

In follow-up discussions with the EPA, reduced asymmetry has been observed from their data if they calibrate the on-board wind measurement on a run-by-run basis, using all data during one particular coast to develop the calibration. Although an improvement was found in the

EPA data using this method, it can lead to incorrect calibration because the vehicle is only in the presence of their track-side anemometry for a short period of time. At all other times during the coast-down, the winds experienced by the track-side and on-board measurements are not the same and this can lead to additional errors in the calibration. The site used by SwRI is a rural road surrounded by farmland and with little or no road-side obstacles. It is feasible that the mean wind-speed profile is well developed and consistent over large distances, providing a reasonable calibration of the on-board device during a full coast. This, however, would not be the case in many geographic locations, and in particular for the Motor Vehicle Test Centre which is embedded in a forested area with clearings for the various road surfaces. This method can therefore not be used for the current test campaign, or as a general procedure.

For a general coast-down or constant-speed scenario, calibration between the 2 m track-side and 5 m on-board measurements are only valid for negligible wind conditions. To eliminate or reduce this error, it is recommended that the on-board wind-measurement device measure the winds at mid-height (approx 2 m) of the vehicle. The coast-down testing for the Phase 1 GHG regulations made use of on-board anemometers at 2 m height which, if calibrated appropriately against ground-based anemometers in close proximity to the track (not the case for those tests), would provide a more consistent calibration. Tanguay (2012) describes such approach based on the Phase 1 data set. Another option that would eliminate the need for calibration altogether is the use of the Free-Stream Anemometer (FSA) under development through a collaboration between NRC, TC, and other parties, which is an on-board instrument that will non-intrusively measure the wind speed and direction at vehicle mid-height sufficiently far forward of the vehicle such that the vehicle proximity does not influence the winds (Tanguay, 2015).

5.3 Comparison of Track Results to Wind Tunnel Results

Recently, the NRC conducted some research to improve the wind-tunnel simulation of heavy-duty vehicles using the 30%-scale truck model that had been previously developed in collaboration between NRC and TC. As part of the recent exercise, the three vehicle configurations tested on the track as part of the current test program were replicated in the wind tunnel. The 30%-scale trailer, side-skirts, and boat-tail models well represented the track-test configurations. The tractor, although configured in a similar manner and with the same tractor-trailer gap distance, does not represent the same tractor tested. The wind-tunnel model is based on as International ProStar with a short sleeper-cab (long sleeper-cab tested on the track) and with strategically redesigned component such as the roof fairing and bumper so as not to represent the OEM tractor. Despite these differences, there is not expected to be a significant difference in the drag performance of the tractor between the track-tested and wind-tunnel-tested versions (within 5%).

The results of the wind-tunnel test-campaign are compared to the results of the coast-down and constant speed tests in Figure 5.4. Good agreement is found in the magnitude of the near-zero-yaw $C_D A$ values for all three configurations. This agreement in results provides added confidence that improvements to track-based and wind-tunnel-based test methodologies are converging to the same results, and can be used in complimentary manner for evaluation of

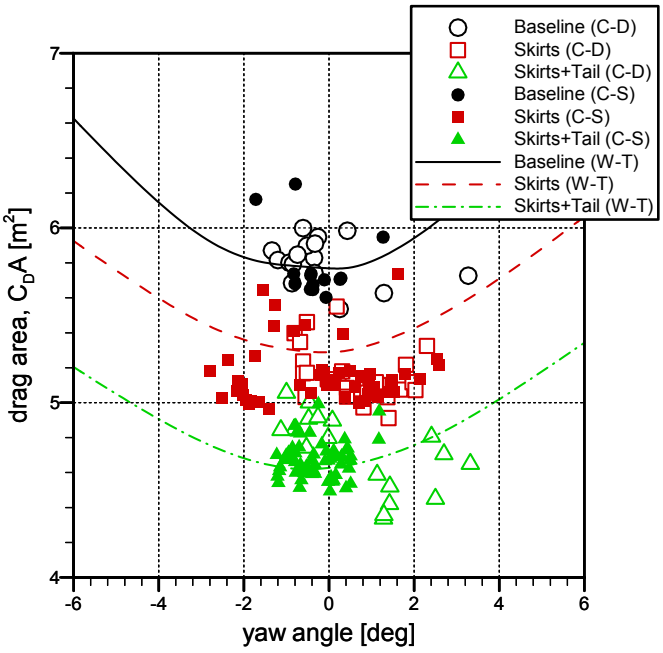

Figure 5.4: Comparison of coast-down, constant-speed, and wind-tunnel results for C_DA with yaw angle.

heavy-duty-vehicle aerodynamics. As proposed by the EPA for the Phase 2 GHG regulations, secondary methods such as wind-tunnel and CFD are to be used to define wind-averaged-drag information for use in the GEM to estimate GHG emissions. The good agreement between results of Figure 5.4 indicate that only small calibration factors are required to relate the NRC high-fidelity wind-tunnel method to the reference coast-down method for zero-yaw C_DA values. Further work is required to validate the yaw characterization of the wind tunnel results.

6. Summary and Conclusions

Through its ecoTECHNOLOGY for Vehicles program, Transport Canada commissioned the National Research Council Canada to perform coast-down and constant-speed tests of a tractor-trailer combination to support regulatory development efforts of Environment and Climate Change Canada and the US Environmental Protection Agency towards reducing greenhouse gas emissions from heavy-duty vehicles. Testing was performed at the Motor Vehicle Test Centre in Blainville, Quebec, in October 2015 using an International ProStar long-sleeper tractor paired with a tandem-axle Manac 53 ft dry-van trailer. Testing was conducted with two trailer-installed drag reduction technologies: a set of side-skirts and a boat-tail. A GPS-based vehicle-speed measurement was combined with track-side and on-board wind anemometry for the coast-down testing, and an additional drive-shaft torque meter was used for the constant-speed testing.

Important findings from the work are:

1. The track surface of the "Bravo Track" at the Motor Vehicle Test Centre is in poor condition. Large bumps in the surface cause vibrations of the vehicle which resulted in reduced data quality. Filtering with a 0.1 Hz low-pass filter was required to eliminate the influence of the bumpiness on the measurements, which limited the ability to adequately resolve wind-gust-related effects on the vehicle road load.
2. The redundancy of using of four track-side sonic anemometers to calibrate the on-board wind measurement (fast-response pressure probe) provided a higher-quality calibration than otherwise would have been possible with a single track-side measurement, thus leading to $C_D A$ measurements with higher precision.
3. The location of the on-board wind measurement (1 m above the front face of the trailer) introduces error in the calibration of the wind-speed and direction experienced by the vehicle. The change in the speed of the terrestrial winds with height has been shown, conceptually, to adversely affect the results of coast-down or constant-speed test results.
4. The rolling resistance of heavy-duty truck tires changes with speed during a coast-down process (more than 30% higher at 100 km/h than at near-zero speed) and has been modeled with an analytical expression for ease of use in coast-down analysis methods. The inclusion of this speed-dependent rolling resistance reduces the calculated $C_D A$ values by up to 10%.
5. Analytical expressions for the mechanical resistance of the drive-axle differentials during coast-down have been developed based on limited data provided by the EPA. The results do not show significant sensitivity to different forms of the analytical model fit to the data.
6. Results from the the coast-down tests, analyzed with the EPA-proposed high/low iteration method, are within 5% of the EPA values for the low-yaw drag area ($C_{D0} A$).
7. Reducing the low-speed range for the high-low-iteration method from 40-24 km/h (25-

15 mph) to 24-8 km/h (15-5 mph) changes the results of the coast-down analysis (higher C_DA values), by minimizing the influence of the aerodynamic contributions to road load at low speeds, thus leading to C_DA measurements with higher precision.

8. Results from the EPA-proposed high/low iteration method compare well to those calculated using a more conventional regression analysis technique (average C_DA within 0.2% for both techniques).

9. The constant-speed method provided significant scatter in the results of C_DA and required additional restrictions on data validity to provide confidence in the data. These additional restrictions eliminated the higher yaw-angle data that were supposed to be the benefit of the constant-speed over the coast-down method.

10. The response of the vehicle cruise control system to changes in the environment and track grade introduced uncertainty in the constant-speed results that required elimination of significant periods of usable data.

11. Good agreement in the estimated zero-yaw drag-area ($C_{D0}A$) between the coast-down results and constant-speed results (with additional restrictions to the constant-speed analysis) that were within 1% for each vehicle configuration.

12. The results of the track tests also compare well to wind-tunnel results of similar vehicle configurations.

The results of this study have demonstrated the ability to obtain good agreement for the aerodynamic performance of a heavy-duty vehicle based on two different road-load methods. This was accomplished with considerable evaluation and re-evaluation of the data in order to understand and account for the numerous sources of error and uncertainty in the measurements of the vehicle and the environment in which the vehicle was operated. These on-road test methods therefore offer the advantage of real-world conditions under which to gather data, however more attention to detail than anticipated is necessary in order to keep uncertainties low and ensure that data are accurate.

References

Cooper, K. R. (1999), "Improving the Wind Tunnel Simulation of Surface Vehicles and the Interpretation of Wind Tunnel Data," , *SAE Conference*, Detroit.

Fontaras, G., Dilara, P., Berner, M., Volkers, T., Kies, A., Rexeis, M. and Hausberger, S. (2014), "An Experimental Methodology for Measuring of Aerodynamic Resistances of Heavy Duty Vehicles in the Framework of European CO_2 Emissions Monitoring Scheme," SAE Int. J. Commer. Veh., **7(1),** doi:10.4271/2014-01-0595.

Luz, R., Rexeis, M., Hausberger, S., Jajcevic, D., Lang, W., Schulte, L., Hammer, J., Lessmann, L., van Pim, M., Verbeek, R. and Steven, H. (n.d.), "Development and validation of a methodology for monitoring and certification of greenhouse gas emissions from heavy duty vehicles through vehicle simulation - Draft Final Report," European Commission Report No. I 07/14/Rex EM-I 2012/08 699, *European Commission*.

McAuliffe, B. R. and Kirchhefer, A. (2015), "Improving the Aerodynamic Efficiency of Heavy Duty Vehicles: Commissioning of the Road Turbulence System and the 30% Scale Tractor-Trailer Model," NRC Report No. LTR-AL-2015-0274, *National Research Council Canada*.

SAE J1263 (2010), "Road Load Metasurements and Dynamometer Simulation Using Coast-down Techniques," Surface Vehcile Recommended Practice No. J1263.

SAE J2263 (2008), "Road Load Metasurements Using Onboard Anemometery and Coastdown Techniques," Surface Vehcile Recommended Practice No. J2263.

SAE J2452 (2008), "Stepwise Coastdown Methodology for Measuring Tire Rolling Resistance," Surface Vehcile Recommended Practice No. J2452.

Tanguay, B. (2012), "A novel technique for predicting free-stream velocity from ground-based anemometric measurements for the aerodynamic assessment of road vehicles during track tests," NRC Report No. LTR-AL-2012-0114, *National Research Council Canada*.

Tanguay, B. (2015), "Summary of the performance of the NRC free-stream anemometry system," NRC Report No. LTR-AL-2015-0071, *National Research Council Canada*.

U.S. Environmental Protection Agency and U.S. Department of Transportation (2011), "Greenhouse Gas Emissions Standards and Fuel Efficiency Standards for Medium- and Heavy-Duty Engines and Vehicles," US Federal Register, **76(179)**, pp. 57106–57513.

U.S. Environmental Protection Agency and U.S. Department of Transportation (2015), "Proposed Rulemaking for Greenhouse Gas Emissions and Fuel Efficiency Standards for Medium- and Heavy-Duty Engines and Vehicles - Phase 2: Draft Regulatory Impact Analysis," EPA Document No. EPA-420-D-15-900.

Wood, R. (2012), "A Review of Reynolds Number Effects on the Aerodynamics of Commercial Ground Vehicles," SAE International Journal of Commercial Vehicles, **5**, pp. 628–639.